

Effects of Paternal Obesity on the Metabolic Profile of Offspring: Alterations in
Gastrocnemius Muscle GLUT4 Trafficking and Mesenteric Adipose Tissue
Transcriptome

A dissertation presented to
the faculty of
the College of Arts and Sciences of Ohio University

In partial fulfillment
of the requirements for the degree
Doctor of Philosophy

Xinhao Liu

August 2018

© 2018 Xinhao Liu. All Rights Reserved

This dissertation titled
Effects of Paternal Obesity on the Metabolic Profile of Offspring: Alterations in
Gastrocnemius Muscle GLUT4 Trafficking and Mesenteric Adipose Tissue Transcriptome

by

XINHAO LIU

has been approved for
the Department of Biological Science
and the College of Arts and Sciences by

Felicia V. Nowak

Associate Professor of Biomedical Science

Joseph Shields

Interim Dean, College of Arts and Sciences

ABSTRACT

LIU, XINHAO, Ph.D., August 2018, Molecular and Cellular Biology

Effects of Paternal Obesity on the Metabolic Profile of Offspring: Alterations in Gastrocnemius Muscle GLUT4 Trafficking and Mesenteric Adipose Tissue Transcriptome

Director of Dissertation: Felicia V. Nowak

Parental obesity increases the risk of obesity in offspring. The overall hypothesis of this work is that offspring inherit altered epigenetic marks from parents that are obese due to consumption of high fat diet (HFD). The first specific hypothesis was that decreased GLUT4 synthesis or impaired trafficking to plasma membrane occurs in insulin resistant HFDO. This study measured expression of total glucose transporter 4, (GLUT4), the major insulin-stimulated transporter of glucose into muscle and adipose cells, as well as its subcellular distribution in the gastrocnemius muscle. The data showed that the level of total GLUT-4, as indicated by a 46kd protein band, exhibits no difference between LFDO and HFDO at 1.5, 6 or 12 months. However, when data from animals of all ages are combined, total GLUT4 expression is significantly higher in female than male HFDO, suggesting that females are protected from IR at least initially by increased GLUT4 expression facilitating increased glucose transport into skeletal muscle. In contrast, male HFDO have higher plasma membrane GLUT4 expression when compared to male LFDO,

suggesting a mechanism in skeletal muscle in males to alter GLUT4 subcellular distribution and prevent worsening of IR.

It was next hypothesized that adipose tissue, as an endocrine organ that secretes multiple adipokines, also contributes to IR. Male HFDO also have increased body fat and increased weight of white adipose tissue (WAT), including mesenteric, subcutaneous, gonadal and retroperitoneal depots. Thus, the second specific hypothesis was that altered production of certain adipokines occurs in insulin resistant HFDO. Data showed that cytokines that increase the risk of IR such as IL1b and Fam3b were increased in male HFDO. Ingenuity Pathway Analysis (IPA) analysis showed that differentially expressed genes (DEGs) were enriched in pathways related to lipid metabolism, endocrine function and multiple organ injuries, such as liver and kidney injuries. This study also characterized the transcriptome of adipose tissue and explored the DNA methylation status of CpG islands located in the promoter regions of several DEGs. However, no DNA methylation differences were detected among these genes, suggesting that the observed differential expression is associated with other epigenetic modifications such as modification of non-coding RNAs and microRNAs. The sex-specificity of strategies in offspring to maintain metabolic balance and resist development of IR strongly suggests that epigenetic mechanisms have been set into play by the metabolic status of their obese HFD-fed sires.

In conclusion, sex-specific strategies in offspring were identified to maintain metabolic balance and resist development of IR. GLUT4 expression was increased in female offspring and translocation to the active site in plasma membrane was increased in HFDO males. RNA sequence analysis revealed altered expression of specific genes in mesenteric adipose tissue in HFDO males that may contribute to the observed IR. Epigenetic analysis showed that DNA methylation was not the mechanism affecting the DEGs studied.

ACKNOWLEDGMENTS

The PhD education at Ohio University is an important milestone of my life. I learn precious knowledge that I will benefit from in my future career, and more importantly I gain a better mindset of research. I received great help and guidance from the people around me to whom I am genuinely grateful.

First of all, I would like to give my most sincere appreciation to my advisor Dr. Nowak whom I have been working with for five years. I was able to choose the research project and design the study freely. And I received great help from her in developing a challenging method for the study. She gave me the intellectual guidance in research with great patience and cares about me in life. With her tremendous help, I was able to get financial support from University to collaborate with colleagues at the University of Massachusetts Medical School where I got to know great scientists and learn new techniques which allowed me to complete my project. Also Dr. Nowak has made every effort to be supportive of my physician scientist career plan.

I would like also to express my sincere appreciation to Dr. Leslie Consitt, Dr. Xiaozhuo Chen and Dr. Allan Showalter. Dr. Consitt has similar research field with me, so she provided me great research insight. I would like to thank Dr. Chen who gave me precious guidance in solving technical issues. Dr. Allan Showalter is considerate to join my committee.

I would like to thank Dr. Yuriy Slyvka for editing my manuscript with insightful comments and Jie Xiang for assisting me in completion of the most laborious part of my research project.

Last but not the least, I would like to express my genuine gratitude to my family. My mother, Lan Liu, my grandmother, Shufang Duan, and my grandfather, Qikui Liu, granted me the genuine support during my Ph.D. study. Their understanding and support are priceless.

TABLE OF CONTENTS

	Page
Abstract.....	3
Acknowledgments	6
List of Tables.....	10
List of Figures	11
List of Abbreviation	12
Chapter 1: Background	14
1.1 Introduction to Obesity	14
1.1.1 Genetic Regulation of Obesity.....	15
1.1.2 Epigenetic Regulation of Obesity	20
1.2 Introduction to the Effects of Parental Obesity.....	23
1.2.1 Effects of Maternal Obesity	25
1.2.2 Effects of Paternal Obesity	26
1.3 Development of Insulin Resistance in Offspring of Obese Sires.....	28
1.3.1 Relationship of Insulin Resistance and Adipose Tissue.....	28
1.3.2 Epigenetic Mechanisms of Adipokine Regulation.....	29
1.3.3 Relationship of Insulin Resistance and Muscle	30
1.3.4 Epigenetic Mechanisms of Muscle Insulin Resistance.....	33
1.4 Project Summary.....	33
Chapter 2: Materials And Methods.....	36
2.1 Chemicals and Solutions	36
2.2 Animal Care And Use	36
2.3 Glucose Tolerance Test (GTT)	37
2.4 Insulin Resistance Index	37
2.5 Total GLUT4 Sample Preparation.....	37
2.6 Fractionated GLUT4 Sample Preparation.....	38
2.7 Analysis of Proteins by Immunoblot.....	39

2.8 RNA Extraction, Library Construction and RNA Sequencing	40
2.9 RNA Sequencing Analysis	42
2.9.1 Sequence Data Quality Control	42
2.9.2 Read Alignment and Gene Abundance Estimation	42
2.9.3 Differential Gene Expression Analysis	43
2.9.4 Ingenuity Pathway Analysis.....	43
2.10 Quantitative RT-PCR Analysis	44
2.11 DNA Extraction of Adipose Tissue from RNA Extracted Trizol Remnant	47
2.12 DNA Bisulfite Conversion	47
2.13 Primer Design, Pyromark PCR and Pyrosequencing	48
2.14 Statistical Analysis	53
Chapter 3: Results	55
3.1 Metabolic Alterations in Offspring Muscle Associated With Paternal Pre-Conception Diet.....	55
3.1.1 GTT Glucose, GTT Insulin and IRI.....	55
3.1.2 Total GLUT4 Expression	56
3.1.3 Subcellular Distribution of GLUT4 in Gastrocnemius Muscle	60
3.1.4 GLUT4 Levels in Cytosol of Male Offspring.....	62
3.2 Role of Mesenteric Adipose Tissue in Insulin Resistance	63
3.2.1 Transcriptome Analysis of Mesenteric Adipose Tissue	63
3.2.2 Altered Genes in Lipid Metabolism Pathways.....	74
3.2.3 Ingenuity Pathway Analysis (IPA) of Gene Expression	76
3.2.4 DNA Methylation Analysis of DEGs in Adipose Tissue	87
Chapter 4: Discussion	91
4.1 Role of Gastrocnemius Muscle GLUT4 in Insulin Resistance	91
4.2 Adipose Tissue and Insulin Resistance	97
References.....	103

LIST OF TABLES

	Page
Table 1. Primers for Differentially Expressed Genes.	45
Table 2. Pyrosequencing Primers for Differentially Expressed Genes.....	50
Table 3. Part 1: Up-regulated Genes.....	65
Table 4. Ingenuity Pathway Analysis.....	77

LIST OF FIGURES

	Page
Figure 1. Interaction Between Adipose Tissue, Skeletal Muscle and Liver in Obesity-Related Metabolic Abnormalities	16
Figure 2. Overview of Experimental Design.....	34
Figure 3. Workflow of Fractionation Protocol for GLUT4	39
Figure 4. GTT, Serum Insulin and IRI.....	56
Figure 5. Representative Immunoblots for Total and Fractionated GLUT4.....	57
Figure 6. Gastrocnemius Muscle Total Glut4 Expression Normalized to Alpha-Actin.....	59
Figure 7. GLUT4 in Gastrocnemius Muscle Plasma Membrane Fraction Normalized to Pancadherin.....	61
Figure 8. GLUT4 in Gastrocnemius Muscle Cytosol and GSV	63
Figure 9. Heat Map of the Relative Abundance of DEGs in 12-Month Male LFDO And HFDO.....	64
Figure 10. Raw Counts of Differentially Expressed Genes.....	76
Figure 11. Network of Lipid Metabolism, Molecular Transport and Small Molecule Biochemistry	83
Figure 12. Network of Cell Death and Survival, Amino Acid Metabolism and Cellular Function and Maintenance.....	84
Figure 13. Network of Organismal Injury and Abnormalities and Renal Damage	85
Figure 14. Network of Endocrine System Development and Function, Molecular Transport and Small Molecule Biochemistry	86
Figure 15. Mgat3 Promoter Cpg Island Methylation Status.....	87
Figure 16. Pip5k1b Promoter Cpg Island Methylation Status	88
Figure 17. Wnt4 Promoter Cpg Island Methylation Status	88
Figure 18. Areg Promoter Cpg Island Methylation Status.....	89
Figure 19. Dagla Promoter Cpg Island Methylation Status.....	89
Figure 20. Efnb Promoter Cpg Island Methylation Status.....	90
Figure 21. Eno1b Promoter Cpg Island Methylation Status.....	90

LIST OF ABBREVIATION

Abbreviations listed in alphabetic order

* Gene abbreviations that appear only once are spelled out in the main text and are not listed.

AKT: Protein kinase B

CCL2: C-C motif chemokine ligand 2

CCR2: C-C chemokine receptor type 2

CTCF: CCCTC-binding factor

DEG: Differentially expressed gene

DMNT1: Dimethylnucleotide transferase 1

GLUT4: Glucose transporter isoform 4.

GSK: Glycogen synthase kinase

GSV: Glucose storage vesicle

GTT: Glucose tolerance test

HDAC: Histone deacetylase

HFD: High fat diet

HFDO: High fat diet offspring

HOMA-IR: Homeostatic model assessment for insulin resistance

IL1 β : Interleukin 1 beta

IL6: Interleukin 6

IR: Insulin resistance.

IRF: Interferon-regulatory factor

IRI: Insulin resistance index.

IRS: Insulin receptor substrate

IPA: Ingenuity pathway analysis

LFD: Low fat diet

LFDO: Low fat diet offspring

MC4R: Melanocortin 4 receptor

NCOR1: Nuclear receptor co-repressor 1

POMC: Proopiomelanocortin

SMRT: Silencing mediator for retinoid and thyroid hormone receptor

SMYD3: SET and MYND domain containing 3

TNF α : Tumor necrosis factor alpha

TWIST1: Twist-related protein 1

WAT: White adipose tissue

CHAPTER 1: BACKGROUND

1.1 Introduction to Obesity

Obesity and over-nutrition, along with type 2 diabetes are recognized controllable challenges in global health that have developed quickly in the past several decades. In 1960, 13.4% of the population in United States was obese (1). The number has almost tripled, coming to 35.2% in 2014 without discrimination between male and female (1). The prevalence of obesity is currently at 37.7% amongst adults over the age of 20 and 17.2% for children and adolescents in the US (2, 3). Obesity is a disease with many contributing factors, including genetic and epigenetic status, parental effects, accessibility to excessive food, and lack of exercise (4, 5). Interestingly, obesity predisposes to type 2 diabetes, which is also characterized by insulin resistance (IR) (6). In 2013, according to International Diabetes Federation, 381 million people had diabetes. And by 2030, this number is estimated to double because of the rapid incidence (7). Type 2 diabetes comprises 90-95% of people with diabetes in the world, while 5-10% have type 1 diabetes (8-10). Taken together, obesity and type 2 diabetes are two major causes of metabolic disease, especially in developed countries. These metabolic diseases put a great burden on the afflicted individuals, their families and society and thus it is urgent to study the mechanism of obesity and type 2 diabetes with the goal of identifying effective means of prevention and treatment. Here, the latest progress in our understanding of obesity and

type 2 diabetes and the mechanisms by which the occurrence of these diseases in parents can affect offspring will be reviewed.

1.1.1 Genetic Regulation of Obesity

Obesity is defined by elevated body mass index (BMI), which is measured by weight in kilograms over height in meters squared (11). IR can also now be measured by a well-established standard, Homeostatic Model Assessment-Insulin Resistance (HOMA-IR) which is a measure used to describe the beta cell function and to quantify IR (12).

Obesity is characterized by chronic inflammation of adipose tissues and IR (13). As a hallmark of obesity, chronic inflammation of adipose tissue has been investigated intensively. Weisberg found that macrophages infiltrate the fat tissue initially, and then lymphocytes follow and accumulate in the fat tissue (14, 15). Macrophages can be divided into two states, M1 and M2, (16, 17), which can transform into each other. M1 state is pro-inflammatory, while M2 state is found to be protective for adipocytes (18). After macrophages infiltrate into fat tissue, they release cytokines such as tumor necrosis factor- α (TNF- α) and interleukin (IL)-6 which activate the inflammation in neighboring adipocytes (19). Canello and Rausch proposed that hypoxia, which can lead to death of adipocytes, is the reason for the chronic inflammation and a chemokine, named C-C motif ligand 2 (CCL2) is thought to be a key mediator in the inflammatory process (20, 21). Another group found that mice are protected from atherosclerotic lesions after CCL2 or CCR2, the receptor for CCL2, is knocked out (22, 23). More experiments need to be

carried out to demonstrate the role of CCL2 or CCR2. Interferon gamma also plays a role in promoting inflammatory response in adipose tissue via increasing production of TNF- α and activating interferon regulatory factors (IRFs) (24). IRFs can either facilitate transcription of inflammatory factors or repress the transcription of anti-inflammatory factors (24).

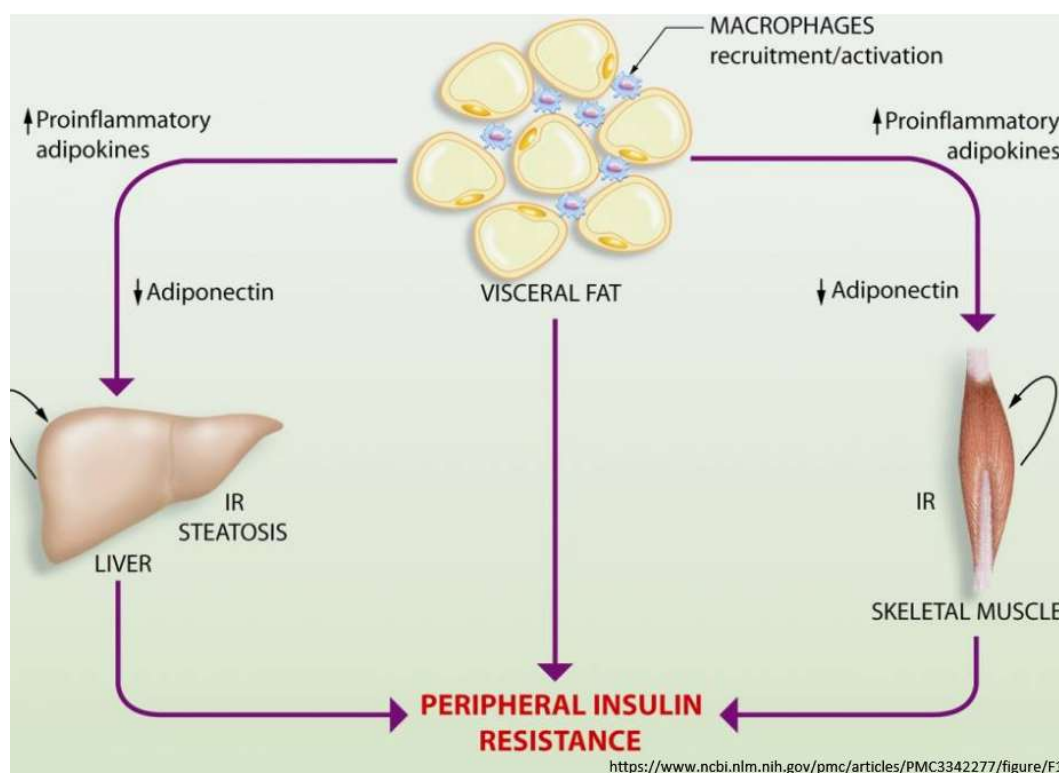


Figure 1. Interaction between adipose tissue, skeletal muscle and liver in obesity-related metabolic abnormalities. Contributors to systemic IR. Expansion of adipose tissue leads to chronic inflammation driven by macrophage infiltration and over production of pro-inflammatory adipokines. Those adipokines lead to peripheral IR whose major contributors are liver and skeletal muscle.

Several mechanisms can contribute to IR from different aspects (Figure 1). IR can present as normal blood glucose with a high level of insulin (hyperinsulinemia) (25). TNF- α is thought by some researchers to be a key mediator in pathophysiology of IR. It phosphorylates insulin receptor substrate (IRS) proteins on serine residues and prevents their interaction with the beta subunit of insulin receptor (26). IL-6 was recently discovered to be involved in IR and its expression by adipose tissue is increased in obesity (27, 28). IL-6 receptor can initiate a signal pathway overlapping with the insulin pathway through modulation of JAK/STAT (29). Activation of JAK leads to activation of STAT which is further translocated into the nucleus to regulate target gene transcription; however, the exact mechanism is unknown (29). On the other hand, it is interesting that adiponectin, a cytokine expressed mainly by adipocytes, actually augments insulin action. The circulating level of adiponectin is reduced in obese people. The level of adiponectin is inversely correlated to liver gluconeogenesis through activation of AMP activated protein kinase (AMPK). AMPK can then inhibit acetyl-CoA carboxylase and two key enzymes involved in gluconeogenesis, phosphoenolpyruvate-carboxykinase and glucose-6-phosphatase (29).

Resistin is a cytokine that was discovered by Steppan et al. in 2001 (30). They investigated the gene expression of resistin and found that resistin levels increased in obese rodents but decreased when thiazolidinedione, an insulin sensitizing medication, was given (30). Moreover, infusion of resistin into lean control animals induced IR (30).

Jackson et al. showed that in mice lacking the resistin gene, fasting glycemia was lower: glucose tolerance and insulin sensitivity were increased while hepatic gluconeogenesis was decreased (31). In addition to adipocytes, monocytes and macrophage produce the largest amount of resistin (31). Resistin gene polymorphisms are believed to contribute to the pathogenesis and susceptibility to obesity in the Egyptian population (32). Genotypes of RETN (Resistin gene) +299AA and RETN-420 GG are significantly associated with obesity as well as with type 2 diabetes mellitus (32).

Impairment in glucose transportation is likely to indicate problems existing in the insulin signaling pathway. Recently, IRS-2, AKT-beta and GSK-3 were shown to play a major role in IR in obese mice (33, 34). IRS proteins, which have several isoforms including IRS-1, 2, 3, are important in insulin signaling. Based on results from gene knockout models, IRS-1 and IRS-2 are the most important in carbohydrate metabolism (35). IRS-1 is involved in IR mostly in muscle and fat tissue (36, 37). IRS-2 is not only associated with IR of muscle and fat, but may also cause beta-cell dysfunction (38). Akt is also a key mediator in the insulin pathway downstream to PI3K that is activated by IRS. An increase of the insulin responsive glucose transporter 4 (GLUT4) mediated glucose uptake is observed with over-expression of Akt (39, 40). Obese mice have an adequate function of Akt-alpha but lose AKT-beta function, showing a decreased insulin sensitivity and consequently having a phenotype that resembles type 2 diabetes mellitus (41, 42). Glycogen synthesis kinase-3 (GSK-3) is a critical enzyme that is inhibited during

glycogen synthesis via Akt phosphorylation (43). Once Akt activation is impaired, GSK-3 will not be inhibited and will thus counteract glycogen synthesis process (44).

Furthermore, expression of a GSK-3 mutant that is resistant to phosphorylation results in impaired hepatic glycogen storage and glycogen synthase activity (45). Expression of GLUT4 is also altered in obesity. Some researchers found that expression of GLUT4 mRNA is downregulated in subcutaneous adipose tissue of obese individuals, and this is considered a major contributor to IR (46). Garvey et al. reported that GLUT4 gene expression is normal in skeletal muscle of insulin-resistant patients with obesity (47). However, wheel running exercise can upregulate GLUT4 expression in obese mice (47).

Both db/db mice whose leptin receptor is mutated and unable to bind leptin and ob/ob mice whose leptin gene is mutated are commonly used as models for type 2 diabetes. The leptin gene was the first gene to be discovered to function alone to protect people from obesity (48). To date, over 40 genetic loci have been associated with obesity. Deletion of fat mass and obesity-associated (FTO) gene, which encodes a nucleic acid demethylase, has been found to lead to increased energy expenditure in mice (49), which implies that FTO decreases energy expenditure. The melanocortin-4 receptor (MC4R) gene, highly expressed in central neuron system, is the most common mutation associated with monogenic obesity. Individuals with a mutation in MC4R exhibit hyperphagia, lack of satiety and decreased energy expenditure. MC4R is activated by gamma-melanocyte-stimulating hormone which is derived from the prohormone precursor

proopiomelanocortin (POMC) and is inhibited by agouti-related peptide (50). Several studies have shown also that alpha-melanocyte-stimulating hormone and agouti-related peptide inhibit each other and transduce opposite signals at the MC4R (51, 52). PPAR-gamma, which encodes the peroxisome proliferator-activated receptor is highly expressed in WAT and brown adipose tissue. It serves as a master regulator of adipogenesis and a potent regulator of lipid metabolism. The insulin sensitizing activity of thiazolidinedione is due to its activation of PPAR-gamma (53-55), leading to inhibition of proinflammatory transcription factors in adipocytes via transrepression (56, 57). For example, E-box transcription factor Twist-related protein 1 (TWIST1) down-regulates the expression of inflammatory genes by forming a complex with a corepressor, silencing mediator for retinoid and thyroid hormone receptor (SMRT) (58). TWIST1 is also regulated by PPAR-gamma, which is reduced in fat tissue in obesity (59, 60).

1.1.2 Epigenetic Regulation of Obesity

Epigenetic changes do not alter the DNA sequence but have a great impact on the transcriptome via a variety of mechanisms including modifying DNA methylation status and chromatin accessibility. In chronic inflammation, coactivators, like cAMP response element binding (CREB) protein/p300 and switching-defective sucrose non-fermenting (SWI/SNF), drive the inflammatory process by activating transcription factors such as NF- κ B, AP-1, and IRFs, the underlying epigenetic mechanism of which is increasing histone acetylation of their promoters (56, 61). By this mechanism, NF- κ B activates its

target genes such as TNF- α and IL-6, thus promoting the inflammatory process (62).

Corepressors such as nuclear receptor co-repressor 1 (NCOR1) and SMRT also are involved in inflammation and assemble multiprotein complexes that contain deacetylases to block transcription (63). Studies of genome wide maps of histone modifications have shown that methylation of lysine 4 or lysine 36 on histone H3 is associated with activation of chromatin, while methylation of lysine 9 and lysine 27 is correlated with repression of chromatin (64). For example, loss of the enzyme Jhd2a, a H3K9 demethylase, may contribute to obesity by altering the expression of metabolism regulating genes (65). CpG island methylation also regulates gene expression as a silencing signal. Bouchard et al. found that DNA methylation status in adipose tissue differs between people who lose weight and people who do not lose weight on a caloric reduction diet (66). Ronn et al. showed that DNA methylation is affected by exercise in both muscle and adipose tissue (67). Exercise also affects SMRT, which suggests that DNA methylation caused by exercise could influence adipocyte inflammation in humans. MicroRNAs (miRs), another class of mediators of epigenetic modification, are also involved in the inflammatory process and differentially expressed in the adipose tissues of lean and obese subjects (67). MiRs are also regulated by levels of circulating inflammatory factors. Interestingly, it has been found that miRs circulate in the blood, which suggests that miRs could be endocrine signaling molecules or biomarkers for obesity or other metabolic disease (68).

IR is also under the epigenetic regulation, through several mechanisms. First of all, the liver is an important organ in the regulation of glucose homeostasis (69). IR is closely associated with the inability of liver to suppress glucose production (70). Clinical data also show that fatty liver is insulin resistant, which is consistent with laboratory data. The PPAR-gamma coactivator 1 α (PPARGC1A) promoter was studied by Sookoian et al. to explore the link between IR and liver dysfunction (71). They found the CpG methylation level of the PPARGC1A promoter to be inversely related to mRNA expression, and positively correlated with Homeostatic model assessment (HOMA)-IR and plasma insulin levels (71). Liver mitochondrial DNA (mtDNA) copy number is a measure of mitochondrial function and metabolic activity; it also is negatively correlated with PPARGC1A promoter methylation status (71). Adipose tissue, previously considered to simply be an energy storage tissue, is now recognized as an endocrine tissue that responds to insulin (72). Epigenetic changes in the promoter of adipose tissue GLUT4 are also related to IR (74). GLUT4 promoter is demethylated during adipocyte differentiation which facilitates nuclear coactivator protein binding to the promoter and insulin sensitivity (73). Presence of CG-rich regions in GLUT4 promoter in Fugu suggests that Fugu GLUT4 gene could be epigenetically regulated (74). MiRs can also regulate GLUT4 expression and translocation in skeletal muscle of an insulin resistant individual (75).

Epigenetic modifications in obesity have an impact on multiple additional genes.

As discussed above, CpG methylation is an important regulatory mechanism that influences adipogenesis and glucose homeostasis (76). When fed a HFD early in life, mice develop hypomethylation in the gene promoter of the satiety-receptor melanocortin-4 receptor (MCR4) but hypermethylation in the gene promoter of the satiety-mediator POMC in the hypothalamus; this demonstrates that methylation patterns can be altered by nutrition (77, 78). Recently, Stepanow et al. found that increased BMI was associated with decreased methylation of exon-1 in melanin-concentrating hormone receptor 1 (MCHR1) in peripheral blood mononuclear cells (79). MCH stimulates appetite which can lead to obesity. According to Campion et al., many variations in DNA methylation at CpG sites of genes that are related to inflammation, adipogenesis and insulin signaling in obesity are consistent with those seen in cancer. This is interesting in light of the known association between obesity and cancer risk (80). MiR expression is different between obese people and lean people, and also differentially regulated between pre-adipocytes and mature adipocytes. Most of the miRs are positively correlated with adiposity and down-regulated in adipocyte differentiation (81). Moreover, glucose metabolism is affected by miRs in subcutaneous adipose tissues. For example, miR-210 is down-regulated in subcutaneous adipose tissues in individuals with type 2 diabetes (81).

1.2 Introduction to The Effects of Parental Obesity

The impact of obesity is not constrained to the individual, but affects the offspring in many ways because of sharing genes and familial environmental (82, 83). Prevalence of childhood obesity tripled between 1980 and 2000 then continued to climb slowly to a current prevalence of 26%, compromising health in this population (1-3). Obese children are at high risk of continuing obesity in adulthood and of developing comorbidities at a younger age that can have immediate consequences, such as dyslipidemia and high blood pressure (84). Obesity not only affects children physically but also mentally. Childhood obesity is associated with decreased ability to regulate cognitive control networks (4). The degree of childhood obesity is positively related with risk of metabolic syndrome, type 2 diabetes, and early onset of atherosclerosis (85). Children with severe obesity also have increased risk of early kidney injury, which manifests as decreased kidney function and increased expression of biomarkers of kidney injury (86). Although genetic factors are important for obesity transmission through generations, dietary and other environmental factors are also critical as they can lead to epigenetic modification, rapidly altering the transcriptome and phenotype (5).

Another important aspect of the epigenetics of obesity is the impact of parental obesity on offspring. Some studies report that DNA methylation changes can be transmitted to the next generation (87). According to Feinberg et al., methylation status is relatively stable over time in individuals but variable when being transmitted to the next generation (88). For example, in a genome-wide human epigenetic study, DNA

methylation patterns were extremely variable between individuals at 227 regions (VMRs) in peripheral blood mononuclear cells, but in 50% of those regions VMRs within the genome of an individual were stable for approximately 11 years (88). The authors posited that stable epigenetic marks are regulated by genetics and unstable marks are regulated by environmental factors (88). In fact, four stable epigenetic changes, which reside within or near food and energy related genes, are correlated with BMI (89). This study supports the concepts that epigenetic changes can be kept in sperm or eggs and transmitted to offspring and that environmental changes that occur during the prenatal period can also affect offspring.

1.2.1 Effects of Maternal Obesity

Maternal obesity has been under intensive research for many years. Maternal obesity increases risk of fetal macrosomia (5), type 2 diabetes and cardiovascular disease of offspring in their later lives (90). Maternal preconception BMI is strongly associated with increased adiposity of newborn infants (90). Gestational diabetes is also strongly associated with obesity and type 2 diabetes in offspring (91). Mother-child cohort studies have demonstrated that high pre-pregnancy BMI is associated in offspring with elevated leptin, an adipokine which has a role in modulating sympathetic tone in young adults, causing increased blood pressure (91). PPARGC1A gene expression is decreased in obese woman with IR as determined by HOMA (92). This is associated with increased methylation in the promoter region of PPARGC1A in the umbilical cord of fetuses (92).

Maternal high fat diet (HFD) leads to increased expression of Gpx-1 (glutathione peroxidase-1) and decreased expression of Pancreas/duodenum homeobox protein-1 (PDX-1) in islets of 20 week male offspring, which is correlated with deterioration of beta-cell function (93). Maternal obesity is also related to neural tube defects in offspring regardless of ethnicity, maternal age or education status (94). There is solid evidence demonstrating that epigenetic mechanisms during development in utero are affected by maternal undernutrition (95). Evidence includes decreased histone lysine 27 trimethylation, decreased glucocorticoid receptor (GR) promoter methylation, and increased histone H3 lysine 9 acetylation in the hypothalamus of both male and female fetuses (95). The resulting upregulation of GR leads to decreased hypothalamic POMC expression and increased incidence of obesity in offspring (95). In the hippocampus, the mRNA of GR is not changed, indicating that the effects are tissue specific (95). Maternal undernutrition around conception will cause epigenetic changes in hypothalamic neurons of offspring that regulate metabolic balance and this effect can last up to 5 years [94].

1.2.2 Effects of Paternal Obesity

Recently, paternal effects on the epigenetic profile of offspring have also come under investigation. Compared with research in maternal obesity, paternal obesity has received far less attention, despite the fact that a father contributes half of the genetic information to its offspring. The first report in mammals of paternal epigenetic transmission of metabolic abnormalities was published in Nature in 2010 and describes a

rat model in which paternal obesity altered expression of 2492 genes overall and 642 pancreatic islet genes in adult female F1 offspring, leading to beta-cell dysfunction (96). The affected genes are involved in cation and ATP binding, cytoskeleton and intracellular transport; hypermethylation of the interleukin 13 receptor subunit alpha 2 (Il13ra2) gene showed the highest fold difference which was a 1.76-fold increase (96). A pre-diabetic state in male mice, manifesting as IR, can be induced by HFD and treatment with streptozotocin (97). This paternal prediabetic condition also alters epigenetic patterns of insulin sensitivity genes, such as phosphatidylinositol 3-kinase regulatory subunit alpha (Pik3r1) and phosphatidylinositol-4,5-bisphosphate 3-kinase catalytic subunit alpha (Pik3ca), in pancreas and sperm of F1 and F2 generation (generated by mating F1) (97). This result is consistent with the findings of another team who first found that paternal obesity alters the epigenome of sperm of offspring (F1 and F2) and diminishes fertility in both male and female offspring (98). Morita et al. reported that adipocyte Igf2 (insulin-like growth factor 2) and Peg3 (paternally-expressed gene 3), two paternally imprinted genes, contribute to resistance to HFD-induced obesity. Dysfunction of Peg3 is correlated with paternal transmission of HFD-induced obesity and Peg3 knockout mice exhibit increases in body fat (99). Moreover, Igf2 may regulate growth of adipocytes. Fullston et al. reported that HFD induced paternal obesity changes testis expression of 414 mRNAs and 11 miRs that potentially program the offspring health (100). For example, although fathers with HFD-induced obesity did not have altered glucose homeostasis, both male

and female offspring showed impaired glucose tolerance due to IR, and female offspring showed increased incidence of obesity. Male offspring had increased levels of leptin, a hormone that has been associated with protection from obesity. Interestingly, epigenetic marks altered by paternal and maternal obesity in humans can be reversed by weight loss through diet and exercise (101, 102).

1.3 Development of Insulin Resistance in Offspring of Obese Sires

1.3.1 Relationship of Insulin Resistance and Adipose Tissue

In addition to pancreas, insulin sensitivity or resistance is most likely to be related to adipose tissue and muscle hormones and metabolism. Adipose tissue is both a fat depository and endocrine organ that secretes many adipokines that regulate energy metabolism (72). Altered secretion of adipokines can predispose offspring to the development of an insulin-resistant phenotype (103). Chronic inflammation, an important pathologic feature of obesity, is caused by abnormal infiltration of macrophages and excess nutrient load in adipose tissue and leads to adipocyte dysfunction in obese individuals (15). In 1995, the major proinflammatory factor TNF- α was found to be highly up regulated in adipose tissues of obese insulin resistant individuals (104). Subsequently, additional inflammatory factors, such as IL-6, IL-1 β , and CCL2, were also found to be up regulated in the obese state (105). Inflammation also is found in non-adipose tissues, including liver and pancreas (106, 107). Although the level of

inflammation in obesity is modest and local compared to that seen with infection or trauma; chronic release of inflammatory factors from adipose tissue can cause IR.

Adipocytes show impaired insulin signaling and decreased glucose uptake after treatment with TNF- α (108). In response to inflammatory signals, kinases that target insulin receptor substrate 1 (IRS-1) for serine phosphorylation are activated, such as JNK, PKR, S6K, extracellular signal-regulated protein kinase (ERK), and mammalian target of rapamycin (mTOR). This inhibits the insulin signaling pathway (109), and suggests that diverse cellular network responses are altered during obesity-related IR. Insulin signaling depends upon a cascade of reactions, one of which begins with binding of insulin to its receptor and ends with increased synthesis of GLUT-4, which is then available for insertion into the plasma membrane. This pathway can be impeded by activation of TNF- α and IL-6 signaling pathways which leads to serine phosphorylation instead of tyrosine phosphorylation of IRS-1 which impairs subsequent insulin signaling (31). Resistin is also involved in IR. Serum resistin levels increase with obesity in humans, rats, and mice (30).

1.3.2 Epigenetic Mechanisms of Adipokine Regulation

Alterations in epigenetic regulation of cytokine genes, like leptin, adiponectin and TNF- α , have the potential to affect the metabolic status of offspring of HFD-fed fathers. A HFD can induce decreased methylation in the promoter region of leptin in epididymal fat of mice at 12 and 18 weeks and thus increase expression of leptin and reduce appetite

(110, 111). Modification of the histone H3K9 from methylation to acetylation in the adiponectin promoter region, and increased methylation of histone H4K20 in the leptin promoter region, are associated with reduced adiponectin expression and enhanced leptin expression, respectively, in adipose tissue from offspring exposed to a maternal HFD during gestation (112). Methylation of the adiponectin promoter is increased by dimethylnucleotide transferase 1 (DNMT1) in adipose tissues and inhibition of DNMT1 by RG108, a chemical inhibitor of DNMT1, results in increased expression of adiponectin and improved insulin sensitivity (111, 113). Bioinformatic analysis of CpG islands in promoter regions of other obesity-related genes has identified regions with a high density of CpGs in genes implicated in adipogenesis, including human PPARGC1, lipoprotein lipase (LPL), fatty acid binding protein 4 (FABP4), and insulin-like growth factor binding protein-3 (IGFBP3) (102). These findings support the concept that such genes are subject to epigenetic modifications induced by a HFD, and these modifications are then transmitted to offspring. Finally although not transgenerational, it has been shown that exposure to a range of nutritional insults during fetal life leads to metabolic dysfunction and hypertension, which is associated with differentially expressed genes (DEGs), including PPARs in offspring kidney (114). There is also evidence that paternal obesity induced by HFD leads to alterations in retroperitoneal adipose tissue transcriptomes of female rat offspring (115).

1.3.3 Relationship of Insulin Resistance and Muscle

Skeletal muscle, consisting of 80% of the body lean mass, is the largest insulin responsive organ for glucose uptake from the bloodstream. In order to fulfill glucose uptake capability, maintaining the integrity of the IRS-1/PI-3 kinase/AKT pathway is critical. Muscle IR is a key factor in Type 2 diabetes mellitus (T2DM) and obesity and is correlated with increased inhibitory IRS-1 serine phosphorylation and decreased Akt activation (116). As a result, downstream events, such as GLUT-4 translocation from its internal storage organelle, GLUT-4 storage vesicle (GSV), into plasma membrane, will be affected. The insulin responsive glucose transporter, GLUT-4, is a member of the family of glucose transporters in which 14 functional isoforms have been identified [116]. GLUT4 transport in muscle is impaired by a HFD related to an early insulin-signaling defect while GLUT4 expression is normal in soleus muscle (117) (118). Xu et al. has reported that insulin can increase translocation of GLUT4 to plasma membrane in insulin resistant soleus muscle (119). Gao et al. reported that insulin stimulation increases the total number of GLUT4 molecules and decreases the cluster size of GLUT4 in plasma membrane (120).

PGC-1 is a transcription factor that regulates GLUT4 expression.

Hypermethylation in the promoter region of PGC-1 can be induced by HFD and reversed by exercise (121). This suggests GLUT4 expression can be regulated epigenetically.

Muscle also has the constitutive transporter, GLUT-1, and these two transporters facilitate uptake of glucose into gastrocnemius muscle. Additional glucose transporters in muscle

include GLUT3, GLUT6 and GLUT10 (122), but their contributions to basal uptake of glucose by gastrocnemius muscle remains to be established. Interestingly, in the basal state, insulin independent glucose uptake facilitated by GLUT-1 is decreased in insulin resistant individuals, although the mechanism is not yet clear (123). There is evidence that abnormal metabolic events occurring in obese fathers who are insulin resistant can be inherited by their offspring and some offspring do not respond to therapeutic lifestyle changes (124).

A number of genes important for regulation of glucose uptake and metabolism are subject to epigenetic regulation. The GLUT-4 promoter is regulated by chromatin binding factors, such as CCCTC-binding factor (CTCF), specificity protein 1 (SP1), and SET and MYND domain containing 3 (SMYD3), which regulate histone acetylation and SMYD3A, Myocyte Enhancer Factor 2A (MEF2A, SP1), CTCF, which regulate the activity of lysine methyltransferase (125). GLUT-4 promoter is also regulated by DNA methylation at specific CpG sites (126). The insulin gene (INS) is also subject to DNA methylation (126). Mitochondrial DNA modification is also subject to epigenetic regulation and has been recently reported to be related to IR resulting in differential expression of a number of energy metabolism genes, such as cytochrome c oxidase subunit VIIa polypeptide 1 (COX7A1), NADH dehydrogenase (ubiquinone) 1 b subcomplex 6 (NDUFB6), and PPARG coactivator 1 alpha (PGC-1 α). It is reasonable to hypothesize that the IR observed in male offspring of HFD-induced obese sires is

correlated with inheritance of epigenetic changes in some or all of these genes from the obese fathers (127).

1.3.4 Epigenetic Mechanisms of Muscle Insulin Resistance

A HFD can induce obesity by impairing mitochondrial function in skeletal muscle (128). The diet-induced mitochondrial dysfunctions then have a critical role in the development of systemic IR (129). IR in muscle may be related to epigenetic changes such as DNA methylation or covalent histone modifications (130, 131). Insulin sensitivity can be improved by sodium butyrate (NaB), which inhibits class I histone deacetylase (HDAC) activity, and other histone deacetylase (HDAC) inhibitors (132). PPAR γ PGC1 α is expressed in the cell nucleus and later translocated to the mitochondria, resulting in upregulation of mitochondrial DNA transcription and replication (133, 134). DNA methylation of PGC1 α gene reduces its expression in myocytes treated with fatty acids and in type 2 diabetic patients. Reduced expression of PGC1 α is associated with decreased density of mitochondria. NaB has been demonstrated to epigenetically regulate mitochondrial adaptations to diet through nucleosome positioning (135).

1.4 Project Summary

A study was designed to investigate the effects of paternal HFD-induced obesity on metabolism and behavior of offspring. To investigate this, a mouse model of transgenerational paternal transmission of metabolic disease was developed, using C57BL6/N mice (Figure 2). It should be noted that this strain differs from the more

commonly used C57BL6/J mouse in which earlier models of paternal obesity have been developed. In brief, male mice were divided into 2 groups. One group was fed a LFD and the other group was fed a HFD for 12 weeks, from 4 to 16 weeks of age. These mice were subsequently mated with female mice fed the LFD. Offspring of LFD (LFDO) and HFD (HFDO) fathers were kept on regular lab chow.



Figure 2. Overview of experimental design. Illustration of mating method and offspring groups. LFD and HFD-fed sires were mated with LFD female founders. All the offspring were kept on regular lab chow diet. Offspring were euthanized at 1.5, 6 and 12 months of age.

A number of serum components of offspring, including insulin, leptin and glucose, were measured at 1.5, 5-6, and 12 months. Mice were also sacrificed at these

time points and tissues and organs were removed, weighed and frozen for future use. One of the findings was that IR was increased in male offspring at 12 months of age.

The present studies were designed to investigate the mechanism of the observed IR. As skeletal muscle and mesenteric adipose tissue are two major regulators of glucose homeostasis, it was decided to investigate the contribution of these two compartments to the observed increase in IRI. Were there changes in skeletal muscle GLUT4 levels or distribution? Were there alterations in mesenteric adipose transcriptome including adipokines causing decreased insulin sensitivity? The central hypothesis of the present study is that epigenetic changes in adipose tissue genes related to IR and muscle utilization of glucose are key components of the development of IR in male offspring of obese fathers. More specifically, IR, which may be related to excess pro-inflammatory cytokine secretion by adipose tissue or to impaired GLUT-4 levels or translocation to muscle plasma membrane, can be transferred from obese fathers to their offspring (129). In order to test these hypotheses the following experiments were done: 1) Total GLUT4 and subcellular plasma membrane and GSV GLUT4 were quantified in the gastrocnemius muscle. 2) RNA-sequencing of mesenteric adipose tissue of male offspring at 12 months in both LFD and HFD groups. 3) Bioinformatics tools were used to process RNA-Seq data to identify DEGs. 4) Pyrosequencing was used to identify epigenetic alterations in DEGs identified in mesenteric adipose tissue.

CHAPTER 2: MATERIALS AND METHODS

2.1 Chemicals and Solutions

Homogenization buffer was comprised of 50mM Hepes, 10mM EDTA, 100mM NaF, 50mM Na pyrophosphate. Immediately before use the following components were added: Na orthovanadate 10mM, protease inhibitor cocktail (Sigma Aldrich, P8340) (5 μ l/ml), phosphatase inhibitor cocktail I (Sigma Aldrich, P2580) (10 μ l/ml), phosphatase inhibitor cocktail II (Sigma Aldrich, P5726) (10 μ l/ml). Sucrose gradients were composed of 40% sucrose (400 μ l), 35% sucrose (600 μ l), 8% sucrose (600 μ l) and 400 μ l sample from bottom to top, for a total of 2 ml. Each sucrose gradient layer concentration was verified by refractometry (ThermoFisher, ABBE-3L).

2.2 Animal Care and Use

All protocols involving animals were approved by Ohio University's Institutional Animal Care and Use Committee (IACUC). Ohio University animal facilities are Association for Assessment and Accreditation of Laboratory Animal Care (AALAC) approved. Pathogen-free C5BL6/N mice were purchased from Harlan Sprague Dawley (Indianapolis, IN). Starting at 4 weeks of age, F0 (first generation) male and female mice were fed either a low fat diet (LFD, 10% kcal fat, D12450B, Research Diets) or a HFD consisting of 45% kcal fat (D12451, Research Diets, New Brunswick, NJ) for 12 weeks before mating. Each group had eight mating pairs: four male LFD/four female LFD and four male HFD/four female LFD. Only obese males fed the HFD whose body weight was

10-25% greater than age- and sex-matched animals on LFD were included in the HFD group sires. During the eight-day mating period, mice were kept on LFD during mating (8:00 am-8:00 pm) then separated and fed their respective diets from 8:00 pm-8:00 am. Offspring were all maintained on regular chow which is also approximately 10% fat. Three male and three female offspring from each group were euthanized at 1.5, 6 and 12 months of age.

2.3 Glucose Tolerance Test (GTT)

Four male and three female F1 (second generation) animals were tested for glucose tolerance at 1.5, 6 and 11-12 months of age. After a 6 hour fast, 1mg glucose/g of body weight was given by intraperitoneal injection (13). Serum glucose level was measured on tail blood at 0, 15, 30, 60 and 120 minutes after injection using a One Touch glucometer. An additional 50 μ l of blood was collected in heparin-coated capillary tubes at 30 minutes for insulin assay, then centrifuged to separate the cells from the plasma. An ultrasensitive mouse insulin assay was done using ELISA kit (Cat #90080, CrystalChem, Downer's Grove, IL) according to the manufacturer's protocol.

2.4 Insulin Resistance Index

Insulin resistance index (IRI) was calculated based on blood insulin and glucose levels at the 30-minute time point of the GTT. $IRI = [GTT \text{ insulin (ng/ml)} \times GTT \text{ glucose (mg/dL)}] / 10$.

2.5 Total GLUT4 Sample Preparation

The right gastrocnemius muscle was collected, flash frozen and stored in liquid nitrogen. Tissues were homogenized for 20s using Ultratrex (Polytron, Duluth, GA) with 1ml buffer per 100 mg tissue. Then 100 μ l 10% TritonX-100 was added (final concentration 1%) and tissues were homogenized 3 times for 10s, then sonicated 2 times for 3s with 10s interval and 60 amplitude (Ultrasonic processor GE130, probe CV18, Sigma Aldrich, St. Louis, MO). The resulting samples were then incubated on ice for 30 minutes, vortexing 3 times at 10 min intervals. The samples were centrifuged at 15000 x g for 25 minutes at 4C and the supernatant stored at -80C for later use.

2.6 Fractionated GLUT4 Sample Preparation

Figure 3 shows a schematic representation of the subcellular fractionation protocol that was developed to isolate and quantify GLUT4 in plasma membrane, cytosol, and GSV. Gastrocnemius muscle tissue (50 mg) was homogenized on ice using a glass Dounce homogenizer, 50-100 strokes with pestle B followed by 50-100 strokes with pestle A until the homogenate was uniform. Samples were then centrifuged at 800 x g for 10 min at 4C. The supernatant was collected and the remaining pellet was frozen at -80C. Supernatant was then subjected to centrifugation at 12000 x g for 30 min at 4C. This pellet, the plasma membrane containing fraction, was resuspended using 50 μ l homogenization buffer (HB) with 0.1% Triton X-100. Each 400 μ l supernatant was layered on top of a sucrose gradient and centrifuged at 150000 x g (Optima TLX ultracentrifuge, TLS 55) for 1.5h at 4C. Ten fractions of 200 μ l each were collected from

top to bottom for immunoblot analysis. An equal volume (20 μ l) of each fraction was loaded in wells for electrophoresis.

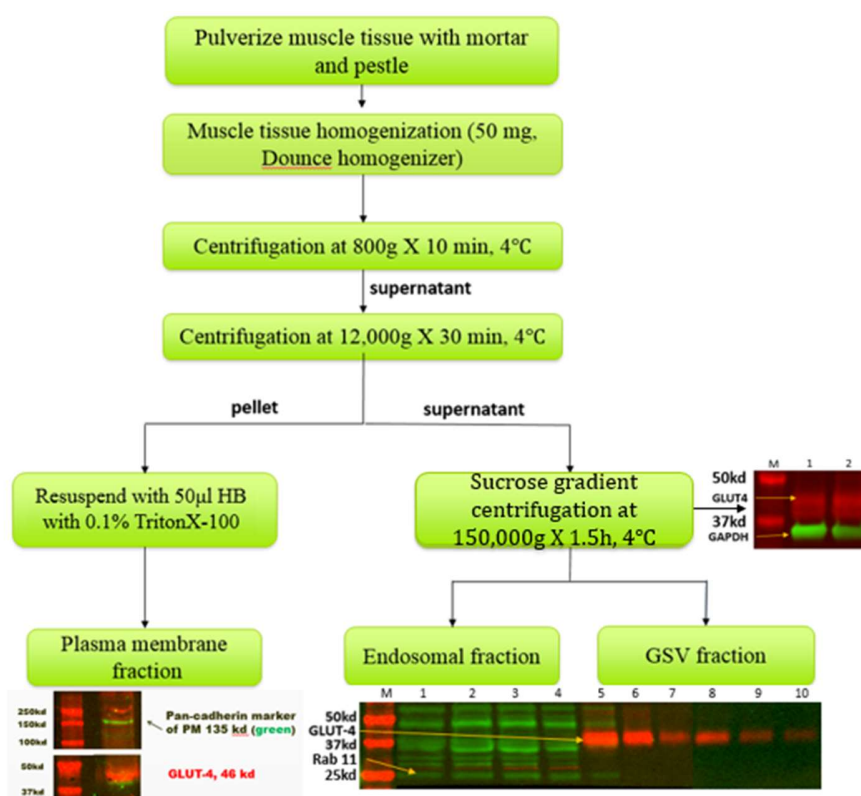


Figure 3. Workflow of fractionation protocol for GLUT4. This protocol allows for GLUT4 localization in plasma membrane, cytosol and GSV from mouse gastrocnemius muscle. No Triton X-100 was added to the initial homogenization buffer.

2.7 Analysis of Proteins by Immunoblot

The protein concentration of each sample was determined by the bicinchoninic acid (BCA) assay (Thermo Scientific BCA Protein Assay Kit). For total GLUT4 analysis, an equal amount of protein (20 μ g) was loaded to 10% polyacrylamide gels (Bio-Rad,

Cat#456-8034) in each well for total GLUT4 quantification. For GLUT4 analysis of subcellular fractions, 20 μ l of each 200 μ l fraction were loaded on 10% polyacrylamide gels. Electrophoresis of both total and fractionated GLUT4 was done on ice using 110 volts for 90 minutes. Licor molecular weight marker (Cat #928-40000) was used. One fraction from each gel was loaded onto a subsequent gel and the signals equalized to allow for quantitative comparisons between gels. Alpha-actin (Santa Cruz, sc-58670) was used as the internal control for total GLUT4 quantification. Pan-cadherin (Abcam, ab22744) was used as plasma membrane marker and internal control for GLUT4 quantification in the plasma membrane fraction. Rab 11(A-6) (Santa Cruz sc-166912) was used as endosome marker. There is no established internal control for GSV fraction. GLUT4 (ThermoFisher, PA1-1065) and Rab 11 primary antibodies were used at 1:2000. Pancadherin was used at 1:500. Goat anti-rabbit (Licor, 926-68071) and Goat anti-mouse (Licor, 926-32210) IRDye were used as secondary antibodies. Image detection was done using an Odyssey Classic scanner (Licor, Lincoln, NE).

2.8 RNA Extraction, Library Construction and RNA Sequencing

Mesenteric adipose tissues from male offspring at 12 months (3 HFDO and 3 LFDO) were homogenized and the cellular RNA was extracted using Trizol Reagent (Sigma-Aldrich, Cat#93289) followed by DNase I treatment using Turbo DNA-free kit (Life Technologies, Cat #AM1907). The detailed protocol was as follows. In brief, 50 mg frozen adipose tissue was homogenized in Trizol using a bullet blender (time set at 3,

speed at 10) (Next Advance, NY). Samples were then centrifuged at 9500 x g for 5 min at 4°C and the Trizol layer (bottom, pink layer) removed with a syringe into a new tube. Then 200 µl chloroform was added and the sample vortexed and centrifuged at 9500 x g for 15 min at 4°C, resulting in three layers, a clear top aqueous layer containing the RNA, an opaque white middle layer containing the DNA and protein, and a pink phenol layer at the bottom. The aqueous layer was removed with a pipette and put into new tube. Then 500 µl isopropanol was added and the sample was briefly vortexed. The aqueous phase was again removed with a P200 micropipette and put into new tube, which was kept at room temperature for 10 minutes, then centrifuged at 9500 x g for 10 minutes at 4°C. One ml 75% ice cold ethanol was added and the sample mixed and centrifuged for 5 minutes at 7500 x g at 4°C. The ethanol was removed and the pellet dried at room temperature for 5-10 minutes. Dried RNA was resuspended in 30 µl diethyl pyrocarbonate (DEPC)-treated water. Total RNA concentration was measured spectrophotometrically using a bio-analyzer (Agilent 2100, Santa Clara, CA). Purified RNA then was subjected to poly (A) mRNA enrichment using NEBnext poly (A) mRNA magnetic isolation module (New England Biolabs, Ipswich, MA). Sample quality was again analyzed with the Bioanalyzer. All samples had an RNA integrity number (RIN) between 1.0 and 4.0. Sequencing libraries were made from 200 pg of poly (A) mRNA with SMARTer® StrandedRNA-Seq Kit (Clontech Laboratories, Mountain view, CA) following standard Illumina protocols. Libraries were pooled and sequenced using an Illumina MiSeq Sequencing System at the

Ohio University Genomic Facility. Paired-end (101 bp) sequencing of 6 libraries (3 LFDO and 3 HFDO) was done across one sequencing lane at first run. Four libraries (2 LFDO and 2 HFDO) were run across one sequencing lane at second run. Five libraries (3 LFDO and 2 HFDO) were run across one sequencing lane at third run. One library (1 HFDO) was run across one sequencing lane at fourth run. Data from all runs were merged into one file of 8 samples from the LFDO and 8 samples from the HFDO for further analysis.

2.9 RNA Sequencing Analysis

All reads generated from the four runs described above were included in the RNA-Seq analysis using the HISAT2-StringTie pipeline (136). Data analysis included sequence data quality control, read mapping, gene abundance estimation, and identification of differentially expressed genes.

2.9.1 Sequence Data Quality Control

Adapter trimming was done by Illumina. Sequence read quality was checked using FastQC (<http://www.bioinformatics.babraham.ac.uk/projects/fastqc>). Per base sequence quality was above 28 and no future trimming was performed.

2.9.2 Read Alignment and Gene Abundance Estimation

The reference genome for mouse (*Mus musculus*, GRCm38) was obtained from HISAT2 website (<https://ccb.jhu.edu/software/hisat2/index.shtml>), file name `gcm38_snp_tran.tar.gz`. The genome annotation gtf file was obtained from Ensembl

(<ftp.ensembl.org/pub/release-84/>), file name Mus_musculus.GRCm38.84.gtf.gz. The short paired-end read sequences (101 bp x 2) were mapped to the reference genome using HISAT2 with default setting. Gene abundance estimation was performed using StringTie with default settings.

2.9.3 Differential Gene Expression Analysis

DESeq2 was used to identify differentially expressed genes following the protocol specified at (<http://ccb.jhu.edu/software/stringtie/index.shtml?t=manual#deseq>). First, gene count matrices were generated using prepDE.py. Then, DESeq Dataset object was created from the count matrices. Lastly, differential expression analysis based on negative binomial distribution was performed using DESeq with default setting. Genes with p-value less than 0.05 between HFDO and LFDO were considered to be statistically significantly different.

2.9.4 Ingenuity Pathway Analysis

List of DEGs and their fold changes were analyzed by Ingenuity Pathway Analysis software. For network analysis, focus molecules are the differentially expressed molecules included in the network. Score indicates the magnitude of the overall change in the network derived from the number of focus molecules and the intensity of differential expression of each of these molecules. Score higher than 50 means there is a strong magnitude of changes. Score lower than 20 means the overall change is of low magnitude. Score between 20 and 50 means there is a medium magnitude of changes.

2.10 Quantitative RT-PCR Analysis

Based on fold changes of DEGs and their possible correlation with metabolism of adipose tissue, for verification of expression, quantitative real-time PCR (qRT-PCR) analysis was performed on a subset of 15 differentially expressed genes identified by RNA-Seq analysis. The 15 genes were selected due to their high fold changes shown by RNA sequencing analysis and/or close relationship to IR and lipid metabolism, for example, adipogenesis. The cDNA synthesis was performed with iScript cDNA synthesis kit (BIO-RAD, Hercules, CA) by incubation of a 20 μ l reaction containing 200 pg of DNase-treated total RNA, 4 μ l of 5x iScript reaction mix, 1 μ l of iScript reverse transcriptase, 1-3 μ l of RNA template and nuclease-free water to a total volume of 20 μ l in a thermal cycler (Eppendorf, Hamburg, Germany) (5 minutes at 25°C, 30 minutes at 42°C, 5 min at 85°C and hold at 4°C). Primers were designed for qRT-PCR using NCBI primer software (NCBI, Bethesda, MD). Detailed information for each primer pair is provided in Table 1. A Stepone plus real-time PCR machine (Applied Biosystems, Foster City, CA) was used to perform the qRT-PCR assays, using 200 pg of total RNA, Power SYBR green PCR master mix (Applied Biosystems, Carlsbad, CA), and 300 nM of each primer pair (IDT, Coralville, IA) in duplicate wells. The cycle time (Ct) for each sample was normalized to the corresponding sample geometric mean of a housekeeping gene [49]. Ribosomal phosphoprotein PO gene, 36B4, was selected as the housekeeping gene. The $2^{-(\Delta\Delta Ct)}$ formula was used to calculate relative abundance of transcripts.

Table 1. Primers for differentially expressed genes

Differentially Expressed Gene	Primer Sequence
Arachidonate 15-lipoxygenase (ALOX15) Ensembl:ENSG00000161905	F: 5'-CCGACCAAGCTG TTCAGGAT-3' R: 5'-TCGCCATCAGCTTCTCCATC-3'
Enolase 1B (ENO1B) Ensembl:ENSMUSG00000059040	F: 5'-CATGGATGTGGCTGCCTCTG-3' R: 5'-AGTTGCAGGACTTCTCGCTC-3'
Interleukin 1 beta (IL1B) Ensembl:ENSMUSG00000027398	F: 5'-TGCCACCTTTTGACAGTGATG-3' R: 5'-AAGGTCCACGGGAAAGACAC-3'
Family with sequence similarity 3, member B (FAM3B) Ensembl:ENSMUSG00000022938	F: 5'-GGTGATAACTCCGGGCCAAT-3' R: 5'-ATTGAGGTCCAAGCACCGTT-3'
Wingless-type MMTV integration site family, member 4 (WNT4) Ensembl:ENSMUSG00000036856	F: 5'-GAATCAACTGCCTCTCGGCT-3' R: 5'-AGAGGAGAGTTTGTGCAGGC-3'
Phosphatidylinositol-4-phosphate 5-kinase, type 1 beta (PIP5K1B) Ensembl:ENSMUSG00000024867	F: 5'-ATCCAGACACAATGGGAGGC-3' R: 5'-CAAATCCCGCTTCTCGTCCT-3'
Amphiregulin (AREG) Ensembl:ENSMUSG00000029378	F: 5'-CAGCTCAGGGAAAGGCGAAT-3' R: 5'-TTCTCCACACCGTTCACCAA-3'
Retinol dehydrogenase 16 (RDH16) Ensembl:ENSMUSG00000069456	F: 5'-GGGACGCAGGAGAACTTGTA-3' R: 5'-AACCAGCAACCCTCATCTTTC-3'

F: Forward primer. R: Reverse primer.

Table 1 continued

Diacylglycerol lipase, alpha (DAGLA) Ensembl:ENSMUSG00000035735	F: 5'-AGGAGCCCACATACTTTGCC-3' R: 5'-GACTTGCTCCTGACACTGCT-3'
Prostaglandin D2 synthase (PTGDS) Ensembl:ENSMUSG00000015090	F: 5'-GGCTCCTTCTGCCCAGTTTT-3' R: 5'-GGGCTGCTGTAGGTGTAGTG-3'
Amphiphysin (AMPH) Ensembl:ENSMUSG00000021314	F: 5'-GACCCTTTCAAGCCCGATGT-3' R: 5'-GCCAAGCCACCTACCATATTC-3'
Occludin (Ocln) Ensembl:ENSMUSG00000021638	F: 5'-GCCATTGTCCTGGGGTTCAT-3' R: 5'-TCGCTTGCCATCACTTTGC-3'
Ephrin B3 (Efnb3) Ensembl:ENSMUSG00000003934	F: 5'-CAAAGGGGGCGTGAGAGACC-3' R: 5'-CCTCTGGTTAGGCACACGC-3'
Mannoside acetylglucosaminyltransferase 3 (MGAT3) Ensembl:ENSMUSG00000042428	F: 5'-CAGCGGACGATGGGATGAAG-3' R: 5'-CGTGGTTGATGTTGATGGCG-3'
Growth hormone releasing hormone (GHRH) Ensembl:ENSMUSG00000027643	F: 5'-GAGCAGAACCTCAATCGGAGAG-3' R: 5'-TCCAGGGTCATCTGCTTGTC-3'
Ribosomal protein, large, P0 (Rplp0) (internal control) Ensembl:ENSMUSG00000067274	F: 5'-GCAGACAACGTGGGCTCCAAGCAGAT-3' R: 5'-GGTCCTCCTTGGTGAACACGAAGCCC -3'

2.11 DNA Extraction of Adipose Tissue from RNA Extracted Trizol Remnant

The remaining aqueous phase overlaying the interphase was removed and discarded and 0.3 ml of 100% ethanol per 1 ml of TRI Reagent (Sigma-Aldrich, St. Louis, MO) was added to the original opaque middle layer from the Trizol extraction. The sample was mixed by inversion, left to settle for 2–3 minutes at room temperature, then centrifuged at 2,000 x g for 5 minutes at 2-8 °C. The resulting DNA pellet was washed using 0.1M trisodium citrate once for 30 minutes followed by 10% ethanol once for 30 minutes (inverting several times every 10 minutes), then centrifuged at 2,000 x g for 5 minutes at 2-8 °C. The supernatant was then discarded. The DNA pellet was dried for 5–10 minutes and dissolved in 8 mM NaOH by repeated slow pipetting with a micropipette, then centrifuged at 12,000 x g for 10 minutes to remove insoluble material and the supernatant transferred to a new tube. Concentrations of DNA were quantified by Qubit (ThermoFisher, Waltham, MA).

2.12 DNA Bisulfite Conversion

DNA methylation kit (Zymo Research, Irvine, CA, Cat #D5001) was used to do the DNA bisulfite conversion. M-dilution buffer (included in kit) was added to 500 ng of the DNA sample and the total volume adjusted to 50 µl with water. After flicking to mix, the samples were incubated at 37°C for 15 minutes. CT conversion reagent (100 µl) (included in kit) was added to each sample followed by incubation in the dark at 50°C for 16 hours. Samples were then placed on ice for 10 minutes. Meanwhile 400 µl of M-

binding buffer (included in kit) was added to a zymo-spin IC column and the column placed into a collection tube. Samples were then loaded onto the columns containing the M-binding buffer. The caps were closed and the columns inverted several times before centrifuging at 12000 x g for 30s. The flow-through was discarded, then 100µl of M-wash buffer was added to each column which was then centrifuged at 12000 x g for 30s. M-desulphonation buffer (200 µl) was added to each column which was then incubated at room temperature for 20 minutes and centrifuged at 12000 x g for 30s. Then 200 µl of M-wash buffer was added and the column centrifuged twice at 12000 x g for 30s. Each column was placed into a 1.5 ml microcentrifuge tube and 20 µl of M-elution buffer was added directly to the column matrix. Columns were centrifuged at 12000 x g for 30s to elute the DNA.

2.13 Primer Design, Pyromark PCR and Pyrosequencing

Promoter regions of 15 selected DEGs were searched and 7 of them were found to have a CpG-rich island. Therefore, forward, reverse, and sequencing primers for regions of interest of the 7 genes were designed manually. The genes and their respective primers are shown in Table 2. The total PCR reaction volume was 25 µl, consisting of 12.5 µl of 2x PyroMark (Qiagen, Hilden, Germany #Cat: 978703) PCR Master Mix, 2.5 µl of 10x Coral Load Concentrate, 0.5 µl of Forward Primer (10µM), 0.5 µl of Biotin tagged Reverse Primer (10µM), 3 µl of RNase-free water, 5 µl of Q-solution, and 1 µl of template DNA (20ng). The protocol for thermal cycling was as follows: 95C for 15

minutes, 45 cycles of 94C for 30s, 55C for 30s and 72C for 30s, then hold at 72C for 10 minutes. PCR products were verified by electrophoresis in 1% agarose gels stained with ethidium bromide and bands visualized using a Bio-Rad fluorescent imager (ChemiDoc XRS+, BIO-RAD). A clean and strong PCR band must be seen before pyrosequencing to ensure the quality of sequencing. Sample preparation for pyrosequencing was done in 96 well plates. Each reaction mixture consisted of 40 μ l bead binding buffer, 3 μ l of streptavidin tagged

Table 2. Pyrosequencing primers for differentially expressed genes

Diacylglycerol lipase, alpha (DAGLA) Ensembl:ENSMUSG00000035735	F: 5'-GAGGTGGTGGAGTTTTGGATTTT-3' R: 5'-AATCCTACTTACTATTTTTTCATCTCC-3' S: 5'-AGGTGGTGGAGTTTTGGAT-3'
Enolase 1B (ENO1B) Ensembl:ENSMUSG00000059040	F: 5'-CATGGATGTGGCTGCCTCTG-3' R: 5'-CTCCACTCTATCTTCCTTTTCCT-3' S: 5'-TAGAAAGGTAGGATAATTT-3'
Amphiregulin (AREG) Ensembl:ENSMUSG00000029378	F: 5'-TAGTTGGGTTTTTGGAGTAGTAAT-3' R: 5'-AACACCTACTACTTTTATAAACCC-3' S: 5'-GTTTTTATTTAGGGTTGGTT-3'
Phosphatidylinositol-4-phosphate 5-kinase, type 1 beta (PIP5K1B) Ensembl:ENSMUSG00000024867	F: 5'-GGTTTGTAGTAGTAGAGTAGT-3' R: 5'-CACCCCTACTCTAAATCCTAA-3' S: 5'-TGTAGTAGTAGAGTAGTT-3'
Mannoside acetylglucosaminyltransferase 3 (MGAT3) Ensembl:ENSMUSG00000042428	F: 5'-ATGGGTGAGTTGATTTTGGAGT-3' R: 5'-TTAAACAATCCCCCACATCT-3' S: 5'-GTGAGTTGATTTTGGAGT-3'
Wingless-type MMTV integration site family, member 4 (WNT4) Ensembl:ENSMUSG00000036856	F: 5'-AAGGTTTATATAGAAAGGTAAGGGGTT-3' R: 5'-CAACTTAAAACAATAACCTAAACTC-3' S: 5'-TATAGAAAGGTAAGGGGTT-3'

Table 2 continued

Ephrin B3 (Efnb3) Ensembl:ENSMUSG00000003934	F: 5'-AATTTTAGTTATTTTGGTGGGTGG-3' R: 5'-AAACTAATTCCTCCCTTAACC-3' S: 5'-AAGAATTTTGTAGGGGT-3'
---	---

F:Forward primer. R: biotin tagged reverse primer S: sequencing primer

beads, 32 μ l of water and 5 μ l of PCR product. Plates were sealed with plastic to prevent spilling and shaken at room temperature for 10 minutes to ensure complete binding of tagged PCR products with streptavidin tagged beads. To prepare the plates for pyrosequencing, 6 sets of 25 μ l of assigned sequencing primers diluted in annealing buffer for four genes, 0.3 μ M per well, were added to a 24 well primer tray. The 24 well tray can accommodate pyrosequencing reactions for 4 genes at a time for each of the 6 samples. Meanwhile, 100 ml each of water, 70% ethanol, denaturation buffer and 1x wash buffer were added to the respective washing trays in the work station. While holding the probe assembly consisting of 24 probes connected to the vacuum pump, the vacuum switch was turned on. First the water was aspirated to rinse the empty probes. The plastic seal was removed from the 96-well plate containing the 24 PCR product-bead mixtures and the probes inserted into the wells for 10 s to draw up the solutions. This allowed the solutions to pass through the vacuum system but the PCR products and beads to be retained on the membrane surfaces at the ends of the probes. The probe assembly was then rinsed by applying sequentially to the tray containing 70 % EtOH for 10 s, then denaturation buffer for 10 s and finally 1 \times wash buffer for 10 s. After all these washing steps, the vacuum system was disengaged and the beads released immediately into the 24 well plate containing the pyrosequencing primers. The PyroMark Q24 Plate containing the samples was heated at 80°C for 2 min on a heat block, then removed and cooled at room temperature for at least 5 minutes. Meanwhile the cartridge was prepared by

injecting the A, C, T, G nucleotides, enzymes and substrates into their respective holding wells. The sequence information was entered into the software of Pyromark software Q24, then the cartridge and the 24 well pyrosequencing plate were inserted into the pyrosequencer (Pyromark Q24) (Qiagen, Hilden, Germany) and the program started.

2.14 Statistical analysis

At least 3 animals/group were used for phenotypic characterization. It was not necessary to exclude any animals due to sickness. The number of mice used in each experiment is indicated in the figure legend. Immunoblots were quantified using Licor Odyssey software (Image Studio v5.2). Multilevel modeling was applied to all comparative analyses of effects of age on GTT glucose and insulin and for all comparisons of IRI. Diet and sex were modeled as the two between-subjects factors and age as the within-subjects factor (137). Main and interaction effects were first tested followed by pairwise comparisons across combinations of diet and sex groups within each age and across ages within each group. Appropriate Bonferroni corrections were applied to adjust p values. Mann Whitney tests were used for analysis of all comparisons of effects of group and sex on GTT glucose and insulin. Data of pyrosequencing were expressed as mean \pm SD. All other data were expressed as mean \pm SEM. Significance was set at $p < 0.05$. GLUT4 total and fractionated values were analyzed as follows: for multiple comparisons, one/two-way ANOVA was used; for analysis between two groups, two-tailed Student's t-test was used. Statistical significance was calculated using

GraphPad Prism (version 6) and accepted as different at $p < 0.05$. For qPCR data, Student's T-test was used to identify significant differences between the LFDO and HFDO phenotypes.

CHAPTER 3: RESULTS

3.1 Metabolic Alterations in Offspring Muscle Associated with Paternal Pre-conception

Diet

3.1.1 GTT Glucose, GTT Insulin and IRI

Glucose levels of 12 month female offspring at 15 and 30 minutes after injection are significantly higher in HFDO when compared to LFDO (Figure 4A). Although the differences are not significant, the glucose levels are lower in HFDO females at 60 and 120 minutes. However, the total area under the curve is not different (18900 in LFDO vs. 18650 in HFDO) (127). Glucose levels of 12-month male offspring at 30 minutes are also higher in HFDO compared to LFDO (Figure 4A). The insulin level at 30 minutes after glucose load is higher in HFDO than in LFDO males at 1.5 months (Figure 4B). Interestingly IRI of male offspring is higher in HFDO than in LFDO at 12 months of age (Figure 4C). The IRI also shows a steady increase with age in HFD sire male offspring (#). IRI in LFDO males also increases with age (**) but only between 1.5 and 6 months. There are also sex differences in IRI at 6 and 12 months, with male offspring having higher IRI values than females. Female offspring also show steadily increasing IRI, but the differences between age groups are not significant.

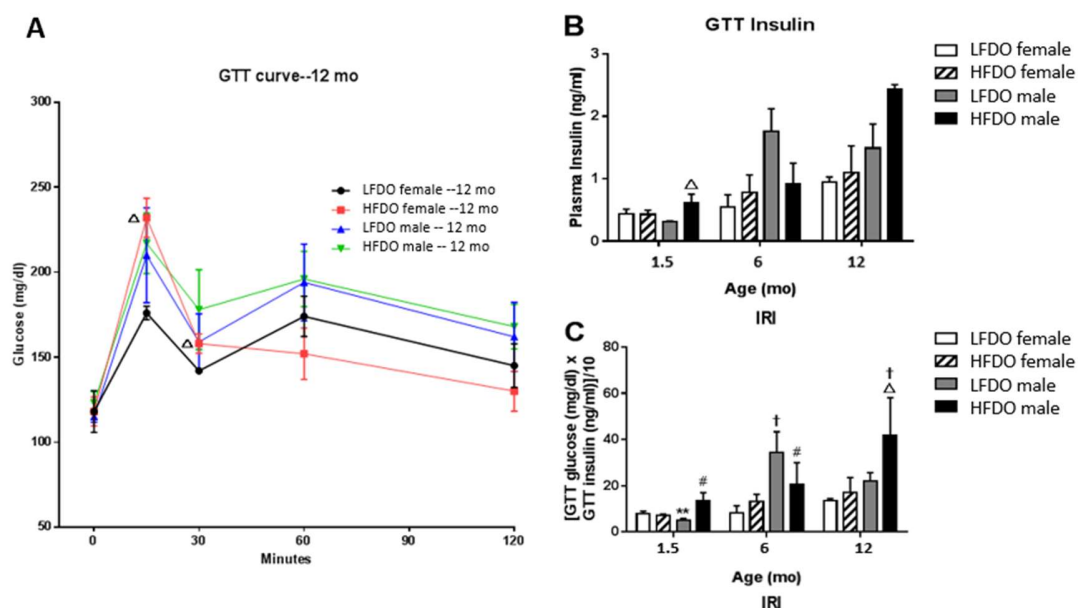


Figure 4. GTT, serum insulin and IRI (A). Glucose levels of 12 month offspring after insulin injection. ●Black line: LFDO Females; ■ Red line: HFDO females; ▲Blue line: LFDO males; ▼Green line: HFDO males. (B) Insulin levels 30 minutes after glucose injection. (C) Insulin resistance index (IRI). (LFDO Females: n=3; HFDO females: n=3; LFDO males: n=4; HFDO males: n=4). Δ: Significantly different from LFDO of the same sex and age ($p < 0.05$); †: Significantly different from HFDO males of the same age ($p < 0.05$); **: significantly different from same sex and diet group at 6 months ($p < 0.05$); #: significantly different from same sex and diet group at 12 months of age. ($p < 0.05$).

3.1.2 Total GLUT4 Expression

In order to investigate the mechanism underlying the increased IRI in male offspring, it was postulated that decreased GLUT4 expression or impaired GLUT4 translocation in muscles were responsible. Total gastrocnemius GLUT4 was measured as well as the distribution of GLUT4 between the cytosol storage vesicles and the plasma

membrane active site. A representative immunoblot for total GLUT4 is shown in Figure 5A.

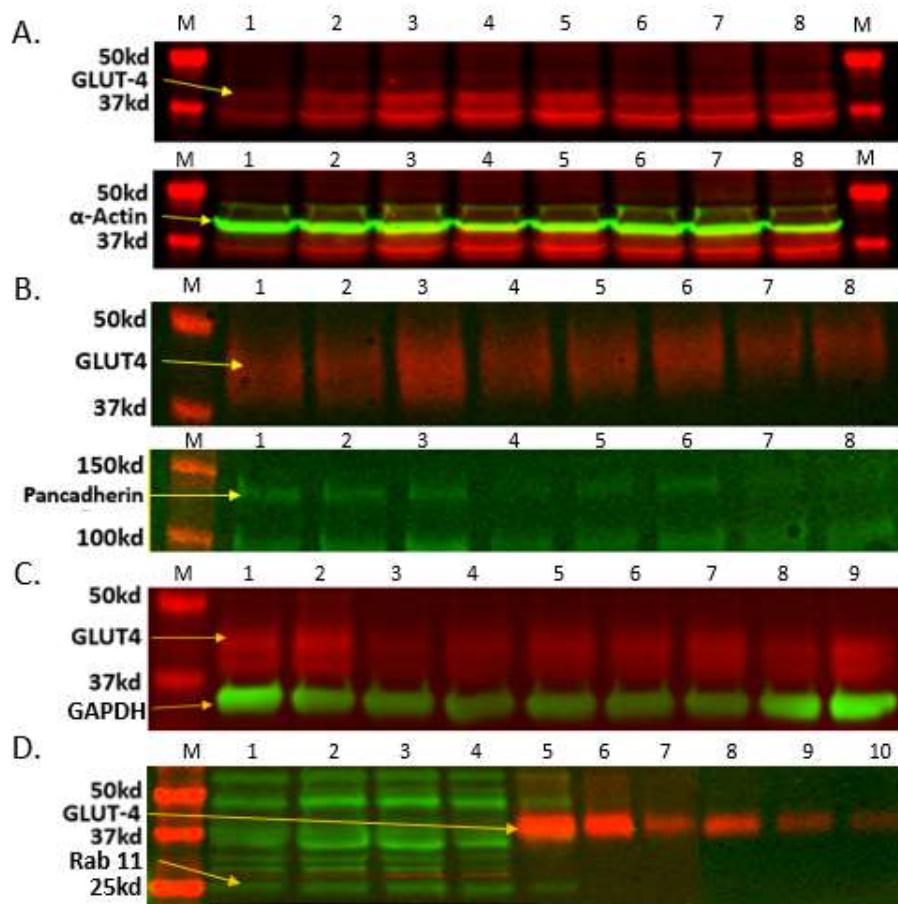


Figure 5. Representative immunoblots for total and fractionated GLUT4. In each section the top panel shows the target protein and the bottom panel shows the control protein for that subcellular fraction. This figure is not intended to show differences between sample groups. All samples were randomly loaded to gels in order to get a reliable image analysis across gels. All values were identified using labels (e.g. F3) which gave no indication of the experimental group (age or diet). These data were only un-blinded when grouped for analysis, at which point the diet groups and sex were revealed. (A) Total cellular GLUT4 and alpha-actin. GLUT4 (Red) (1:2000); alpha-actin (Green) (1:2000); Lane M—molecular weight markers; Lanes 1-8 show individual gastrocnemius muscle samples (F3

LFDO 6-month; F7 LFDO 6-month; F15 LFDO 6-month; F11.3 HFDO 12-month; F3.4 HFDO 12-month; F42 LFDO 1.5-month; F1 LFDO 12-month; F1 LFDO 12-month. (B) Plasma membrane GLUT4. Lanes 1-8 are individual plasma membrane fraction samples (M40 LFDO 1.5-month; M1.6 HFDO 1.5-month; F4.7 HFDO 1.5-month; M2.1 HFDO 12-month; M1.8 HFDO 6-month; M3.6 HFDO 1.5-month; M2 LFDO 6-month; M13 LFDO 6-month). GLUT4 (Red) (1:2000); Pan-cadherin (Green) (1:500); (C) Cytosolic GLUT4. Lanes 1-9 are individual samples of total cytosol (M2.6 HFDO 6-month; M17 LFDO 12-month; M1.8 HFDO 6-month; M3.5 HFDO 12-month; M40 LFDO 1.5-month; M3.1 HFDO 6-month; M56 LFDO 1.5-month; M1.6 HFDO 1.5-month; M2.5 HFDO 1.5-month). GLUT4 (Red) (1:1000); GAPDH (Green) (1:1000); (D) Endosomal and GSV GLUT4. GLUT4 (Red) (1:2000); Rab11 (Green) (1:2000). Lanes 1-10 are separate sucrose gradient fractions (top to bottom) from a single sample (M3.5 fraction 1-10). Numbers in parentheses indicate antibody dilutions. Lanes 8, 9 and 10 are the 8th, 9th and 10th fraction of the same sample run in another gel.

As shown in Figure 6, no significant difference in GLUT4 expression is detected between LFDO and HFDO for either male or female sex, which suggests that total GLUT4 expression is not influenced by paternal obesity. There is no significant difference between age groups which suggests that total GLUT4 expression is steady regardless of age. Interestingly, there are no significant sex differences in total GLUT4 in specific age groups for either LFDO or HFDO (Figure 6A). When data from all age groups are combined, female offspring from both diet groups have higher expression of total GLUT4 than male offspring (Figure 6B).

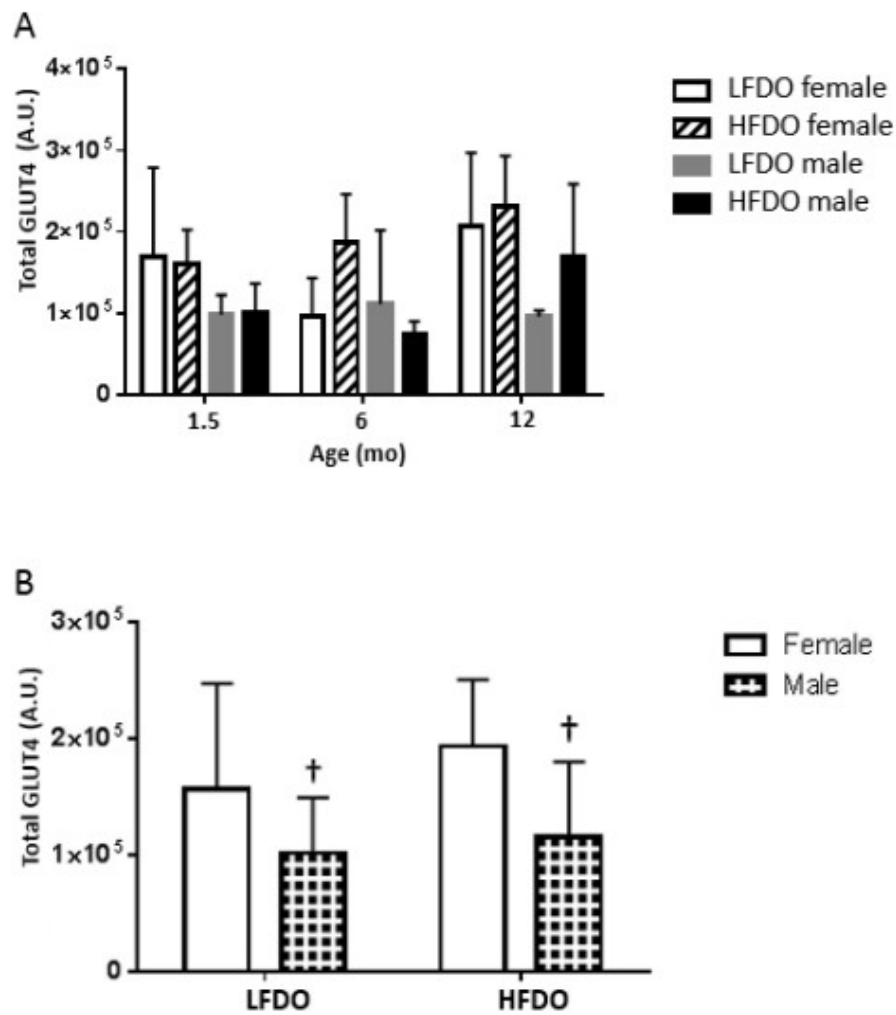


Figure 6. Gastrocnemius muscle total GLUT4 expression normalized to alpha-actin. (A) Total GLUT4 expression in LFDO and HFDO males and females at 1.5, 6, and 12 months (n = 3). (B) Total GLUT4 expression of female versus male offspring, all age groups (n = 9). A.U.: Arbitrary Units. †: significantly different between male and female offspring in LFDO and HFDO (p < 0.05).

3.1.3 Subcellular Distribution of GLUT4 in Gastrocnemius Muscle

Comparisons were initially done separately for each age (Figure 7A). At 12 months HFDO males have higher GLUT4 expression on plasma membrane than LFDO males. However, this difference is not statistically significant. When data from all males are combined (Figure 7B), HFDO have significantly higher GLUT4 expression on plasma membrane than LFDO, suggesting that in males, muscle tissue has developed a mechanism of transferring more GLUT4 to plasma membrane to increase glucose uptake from plasma and prevent hyperglycemia. There are no sex differences in GLUT4 expression on plasma membrane. There are no differences in gastrocnemius muscle GLUT4 levels in LFDO versus HFDO females in individual age groups or when data from all age groups are combined (data not shown).

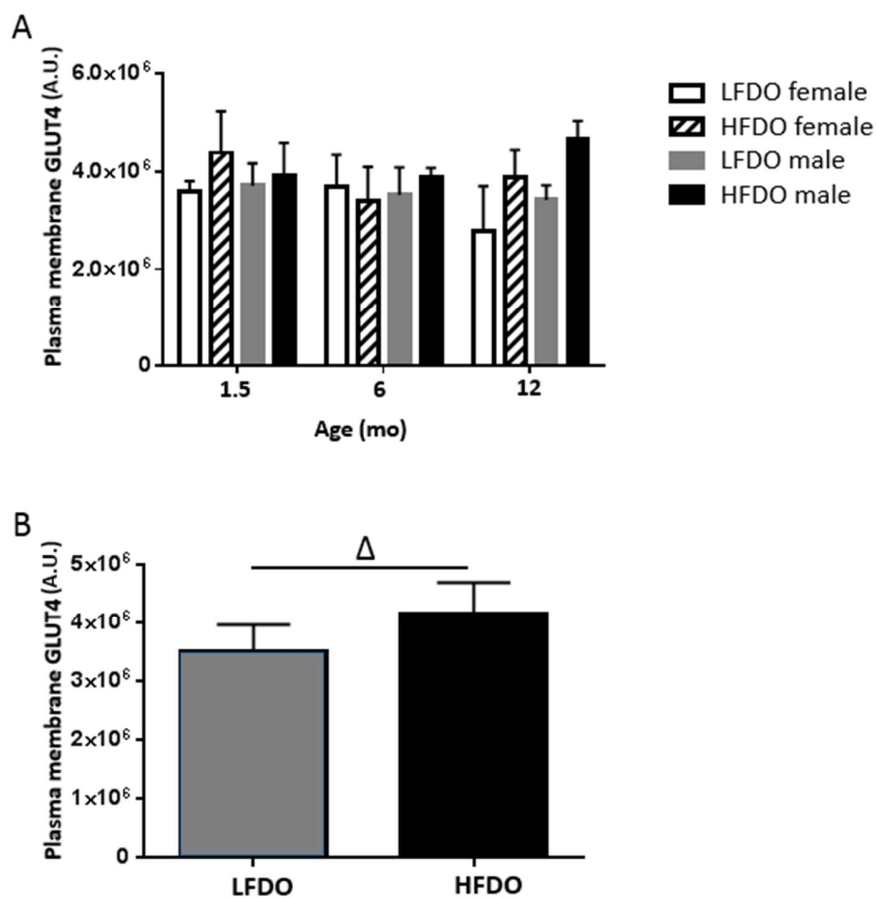


Figure 7. GLUT4 in gastrocnemius muscle plasma membrane fraction normalized to pancadherin. Plasma membrane samples were prepared as described in materials and methods, Fractionated GLUT4 Sample Preparation (A) Gastrocnemius muscle plasma membrane GLUT4 levels in LFDO and HFDO males and females at 1.5, 6 and 12 months of age ($n = 3$). (B) Gastrocnemius muscle plasma membrane GLUT4 levels in LFDO and HFDO males. (LFDO: $n = 9$; HFDO: $n = 9$) (All ages); A.U.: Arbitrary Unit. Δ : Significant difference between LFDO and HFDO ($p < 0.05$).

3.1.4 GLUT4 Levels in Cytosol of Male Offspring

Expression of cytosolic GLUT4 in 12-month male HFDO is only 54% of cytosolic GLUT4 in LFDO males (Figure 8A). Expression of cytosolic GLUT4 in all males is also lower in HFDO when compared to LFDO. These differences did not reach significance (Figure 8B). Expression of GSV GLUT4 in 12-month male HFDO is also decreased to 51% of that seen in LFDO, in close agreement with the results from cytosolic GLUT4 (Figure 8C).

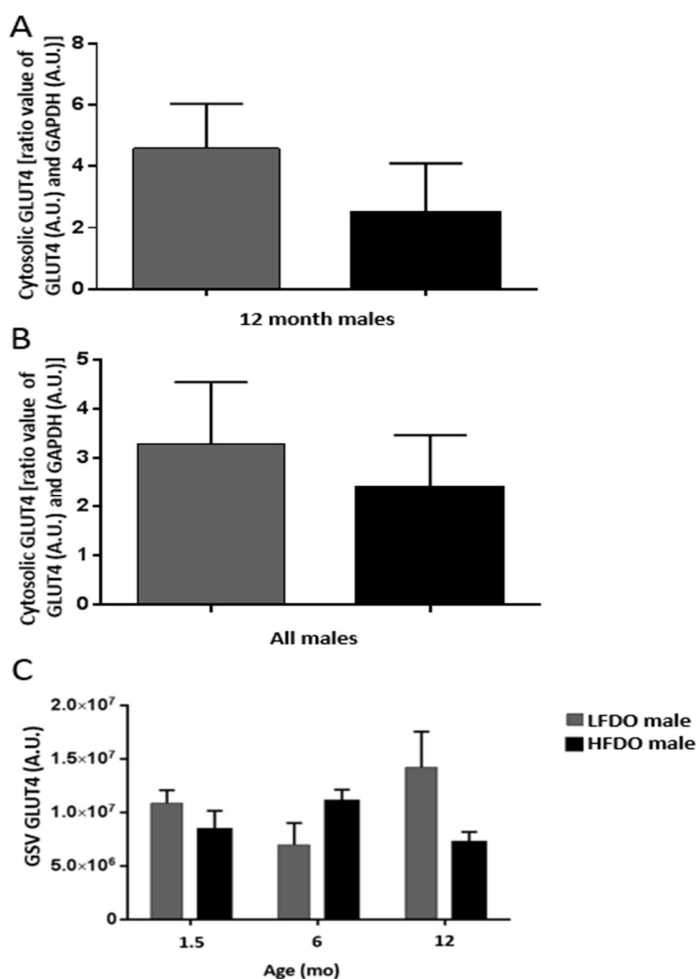


Figure 8. GLUT4 in gastrocnemius muscle cytosol and GSV. Cytosol values were normalized to GAPDH. (A) Cytosolic GLUT4 in male offspring at 1.5, 6 and 12 months of age (LFDO male: n = 3; HFDO male: n = 3) (B) Cytosolic GLUT4 in all male offspring (LFDO male: n = 9; HFDO male: n = 9). (C) GSV GLUT4 in male offspring at 1.5, 6 and 12 months of age (LFDO male: n = 3; HFDO male: n = 3).

3.2 Role of Mesenteric Adipose Tissue in Insulin Resistance

3.2.1 Transcriptome Analysis of Mesenteric Adipose Tissue

It was next hypothesized that the increased IRI in HFDO was due at least in part to the observed increase in % body fat and weight of WAT depots, leading to a metabolic shift in hormones and cytokines secreted by these depots. To investigate which genes and pathways are altered in the mesenteric adipose tissue in offspring of fathers fed the HFD, we analyzed the transcriptome from mesenteric adipose tissue mRNA from three male LFDO and three male HFDO. We identified 192 genes that are differentially expressed at 12 months in HFDO versus LFDO. Of these, 113 genes are up-regulated and 79 genes are down-regulated in the mesenteric adipose tissue from the offspring of HFD-fed fathers. However only 138 of the 192 DEGs are in the ingenuity pathway analysis (IPA) database and can be recognized by IPA software. Table 4 shows the 79 upregulated and 59 downregulated genes in this database. The transcripts form a signature of transcriptomic differences in mesenteric adipose tissue that are affected by the fat content of paternal diet (Figure 9).

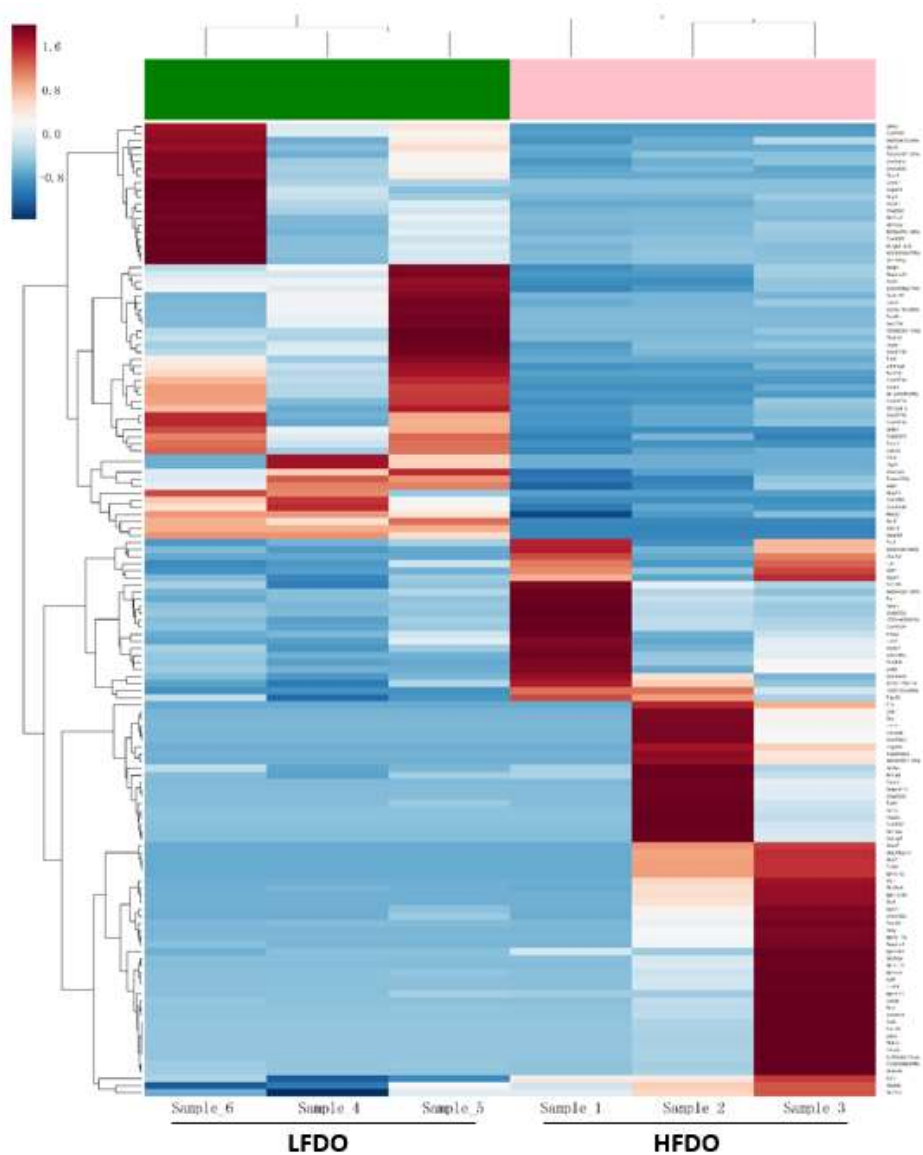


Figure 9. Heat map of the relative abundance of DEGs in 12-month male LFDO and HFDO. From the genes that showed differential expression, the ones with $p < 0.05$ ($n=192$) were plotted in a heat map. Red bars show the up-regulated genes and blue bars show those that are down-regulated.

Table 3. Part 1: Up-regulated Genes

Symbol	Gene Description	Location	Type(s)	Log2 FC	P Value
OCLN	occludin	plasma membrane	other	5.716	0.000497
FAM3B	family with sequence similarity 3 member B	extracellular space	cytokine	5.585	0.000705
SCIN	scinderin	cytoplasm	other	5.479	0.000451
TMPRSS4	transmembrane protease, serine 4	other	peptidase	5.352	0.00123
4933413J09Rik	RIKEN cDNA 4933413J09 gene	other	other	5.263	0.0011
SLC30A2	solute carrier family 30 member 2	plasma membrane	transporter	5.102	0.00221
ACTN2	actinin alpha 2	nucleus	transcription regulator	4.847	0.00416
EDN3	endothelin 3	extracellular space	other	4.793	0.00469
Clec4a4	C-type lectin domain family 4, member a4	plasma membrane	transmembrane receptor	4.699	0.00557
IL1B	interleukin 1 beta	extracellular space	cytokine	4.642	0.0062
VWA3B	von Willebrand factor A domain containing 3B	other	other	4.581	0.00734
ANO7	anoctamin 7	plasma membrane	transporter	4.577	0.00706
Igkv12-89	immunoglobulin kappa chain variable 12-89	other	other	4.566	0.00723
Akr1c19	aldo-keto reductase family 1, member C19	other	other	4.509	0.00822

Table 3 Part 1 continued

PLEKHH1	pleckstrin homology, MyTH4 and FERM domain containing H1	cytoplasm	other	4.456	0.00944
UBE2QL1	ubiquitin conjugating enzyme E2Q family like 1	nucleus	enzyme	4.404	0.0103
Igkv2-112	immunoglobulin kappa variable 2-112	other	other	4.322	0.0119
MMP7	matrix metalloproteinase 7	extracellular space	peptidase	4.253	0.0135
Ighv2-9	immunoglobulin heavy variable 2-9	other	other	4.241	0.00882
DIO1	iodothyronine deiodinase 1	cytoplasm	enzyme	4.238	0.0139
Serpinb1b	serine (or cysteine) peptidase inhibitor, clade B, member 1b	other	enzyme	4.211	0.0149
CDKL1	cyclin dependent kinase like 1	nucleus	kinase	4.103	0.0181
D6Ert527e	DNA segment, Chr 6, ERATO Doi 527, expressed	other	other	4.044	0.0199
B3GALT5	beta-1,3-galactosyltransferase 5	cytoplasm	enzyme	4.002	0.0215
DDC	DOPA decarboxylase	cytoplasm	enzyme	3.969	0.0229
Gm26583	predicted gene, 26583	other	other	3.96	0.0233
Prss30	protease, serine 30	plasma membrane	peptidase	3.929	0.00774
AMPH	amphiphysin	plasma membrane	other	3.927	0.00146
LRTM2	leucine rich repeats and transmembrane domains 2	other	other	3.919	0.0249
GSTA5	glutathione S-transferase alpha 5	cytoplasm	enzyme	3.914	0.0249
MSI1	musashi RNA binding protein 1	cytoplasm	other	3.905	0.0253
PDZD3	PDZ domain containing 3	plasma membrane	transporter	3.885	0.0267

Table 3 Part 1 continued

IGSF23	immunoglobulin superfamily member 23	other	other	3.883	0.0127
Gm19345	predicted gene, 19345	other	other	3.868	0.0272
C1orf106	chromosome 1 open reading frame 106	other	other	3.858	0.0279
RDH16	retinol dehydrogenase 16 (all-trans)	cytoplasm	enzyme	3.815	0.00177
LRRC26	leucine rich repeat containing 26	plasma membrane	ion channel	3.689	0.0362
KDF1	keratinocyte differentiation factor 1	plasma membrane	other	3.689	0.0362
Gm3002	alpha-takusan pseudogene	other	other	3.679	0.037
TRAT1	T-cell receptor associated transmembrane adaptor 1	plasma membrane	kinase	3.611	0.0276
GABRD	gamma-aminobutyric acid type A receptor delta subunit	plasma membrane	ion channel	3.571	0.0435
AREG	amphiregulin	extracellular space	growth factor	3.568	0.0436
TMEM229A	transmembrane protein 229A	other	other	3.567	0.0437
KLK3	kallikrein related peptidase 3	extracellular space	peptidase	3.559	0.0444
Gm17815	lactate dehydrogenase A pseudogene	other	other	3.53	0.0279
Ighv8-12	immunoglobulin heavy variable V8-12	other	other	3.522	0.0466
CACNG8	calcium voltage-gated channel auxiliary subunit gamma 8	plasma membrane	ion channel	3.495	0.0489
A630035G10Rik	RIKEN cDNA A630035G10 gene	other	other	3.494	0.0487
ESM1	endothelial cell specific molecule 1	extracellular space	growth factor	3.488	0.00916

Table 3 Part 1 continued

PIP5K1B	phosphatidylinositol-4-phosphate 5-kinase type 1 beta	cytoplasm	kinase	3.451	0.00293
Gm10548	ribosomal protein L29 pseudogene	other	other	3.416	0.0046
Ces2e	carboxylesterase 2E	other	other	3.415	0.0159
SLC39A4	solute carrier family 39 member 4	plasma membrane	transporter	3.382	0.0139
Gm15925	leukocyte immunoglobulin-like receptor, subfamily A (with TM domain), member 6 pseudogene	other	other	3.22	0.0421
C530008M17Rik	RIKEN cDNA C530008M17 gene	other	other	3.149	0.0377
SLC6A19	solute carrier family 6 member 19	plasma membrane	transporter	3.142	0.0457
5430402O13Rik	RIKEN cDNA 5430402O13 gene	other	other	3.113	0.0153
Igkv4-62	immunoglobulin kappa variable 4-62	other	other	3.017	0.0392
4732440D04Rik	RIKEN cDNA 4732440D04 gene	other	other	2.991	0.0065
9930014A18Rik	RIKEN cDNA 9930014A18 gene	other	other	2.845	0.00855
Gm20033	predicted gene, 20033	other	other	2.801	0.0176
BATF2	basic leucine zipper ATF-like transcription factor 2	other	other	2.707	0.0267
Igkv4-71	immunoglobulin kappa chain variable 4-71	other	other	2.642	0.0293
Gm15326	predicted gene 15326	other	other	2.635	0.0156
FOXC2	forkhead box C2	nucleus	transcription regulator	2.614	0.0327

Table 3 Part 1 continued

LGI4	leucine rich repeat LGI family member 4	extracellular space	other	2.442	0.0284
EVPL	envoplakin	plasma membrane	other	2.399	0.0468
LPIN3	lipin 3	nucleus	phosphatase	2.324	0.0356
SERPINC1	serpin family C member 1	extracellular space	enzyme	2.316	0.0369
RNF165	ring finger protein 165	nucleus	enzyme	2.19	0.044
MYOM1	myomesin 1	cytoplasm	other	2.121	0.0455
ARID5A	AT-rich interaction domain 5A	nucleus	transcription regulator	2.035	0.0494
Tspyl3	TSPY-like 3	other	other	2.005	0.0462
6720427I07Rik	RIKEN cDNA 6720427I07 gene	other	other	1.927	0.0447
F2RL1	F2R like trypsin receptor 1	plasma membrane	G-protein coupled receptor	1.898	0.0289
MGAT3	mannosyl (beta-1,4-)-glycoprotein beta-1,4-N-acetylglucosaminyltransferase	cytoplasm	enzyme	1.895	0.0419
HNRNPF	heterogeneous nuclear ribonucleoprotein F	nucleus	other	1.876	0.0356
MGAT4A	mannosyl (alpha-1,3-)-glycoprotein beta-1,4-N-acetylglucosaminyltransferase, isozyme A	cytoplasm	enzyme	1.753	0.0344
SLC41A2	solute carrier family 41 member 2	plasma membrane	transporter	1.468	0.0485

Table 3 Part 2: Down-regulated Genes

Symbol	Gene Description	Location	Type(s)	Log2 FC	P Value
ENO1	enolase 1	cytoplasm	enzyme	-7.404	3.43E-06
ALOX15	arachidonate 15-lipoxygenase	cytoplasm	enzyme	-5.507	0.000574
STX19	syntaxin 19	other	other	-5.091	0.00174
Gm14769	predicted gene 14769	other	other	-5.083	0.00157
SLITRK4	SLIT and NTRK like family member 4	extracellular space	other	-5.007	0.00196
CAPN11	calpain 11	cytoplasm	peptidase	-4.968	0.0032
EFNB3	ephrin B3	plasma membrane	kinase	-4.832	0.00315
TNNC2	troponin C2, fast skeletal type	cytoplasm	other	-4.723	0.00403
BCL2L10	BCL2 like 10	cytoplasm	other	-4.683	0.00444
TBX18	T-box 18	nucleus	transcription regulator	-4.418	0.00827
ELAVL4	ELAV like RNA binding protein 4	cytoplasm	other	-4.349	0.00988
MUM1L1	MUM1 like 1	cytoplasm	other	-4.334	0.00997
OR12D2	olfactory receptor family 12 subfamily D member 2 (gene/pseudogene)	plasma membrane	G-protein coupled receptor	-4.274	0.0121
Gm5385	3-phosphoglycerate dehydrogenase pseudogene	other	other	-4.197	0.0134
TSHB	thyroid stimulating hormone beta	extracellular space	other	-4.18	0.0137
SEC14L4	SEC14 like lipid binding 4	other	transporter	-4.08	0.0186

Table 3 Part 2: continued

PHYHIPL	phytanoyl-CoA 2-hydroxylase interacting protein like	cytoplasm	other	-3.823	0.027
Gm7291	predicted gene 7291	other	other	-3.81	0.0275
CCDC183	coiled-coil domain containing 183	other	other	-3.74	0.0331
POU1F1	POU class 1 homeobox 1	nucleus	transcription regulator	-3.727	0.0112
Gm12666	predicted gene 12666	other	other	-3.715	0.00706
TNNC1	troponin C1, slow skeletal and cardiac type	cytoplasm	other	-3.697	0.00895
0610009E02Rik	RIKEN cDNA 0610009E02 gene	other	other	-3.689	0.0336
Gm9085	predicted gene 9085	other	other	-3.678	0.016
ASCL2	achaete-scute family bHLH transcription factor 2	nucleus	transcription regulator	-3.677	0.0343
A530083M17Rik	RIKEN cDNA A530083M17 gene	other	other	-3.641	0.00819
Hmgb1-rs16	high mobility group box 1, related sequence 16	other	other	-3.535	0.00653
B230319C09Rik	RIKEN cDNA B230319C09 gene	other	other	-3.489	0.0487
PTGDS	prostaglandin D2 synthase	cytoplasm	enzyme	-3.488	0.049
GHRH	growth hormone releasing hormone	extracellular space	other	-3.488	0.049
SLC24A1	solute carrier family 24 member 1	plasma membrane	transporter	-3.48	0.0495

Table 3 Part 2: continued

NRIP3	nuclear receptor interacting protein 3	other	other	-3.424	0.0271
mir-181	microRNA 181a-1	cytoplasm	microRNA	-3.301	0.0201
ZDHHC24	zinc finger DHHC-type containing 24	plasma membrane	other	-3.285	0.000153
A930003O13Rik	RIKEN cDNA A930003O13 gene	other	other	-3.271	0.0237
Mir155hg	Mir155 host gene (non-protein coding)	other	other	-3.257	0.0392
TMEM255A	transmembrane protein 255A	extracellular space	other	-3.102	0.0112
TEKT1	tektin 1	cytoplasm	other	-3.03	0.0261
8030487O14Rik	RIKEN cDNA 8030487O14 gene	other	other	-3.023	0.0434
Gm20594	predicted gene, 20594	other	other	-2.939	0.0247
EMP1	epithelial membrane protein 1	plasma membrane	other	-2.927	0.00619
Gm15712	ribosomal protein L3 pseudogene	other	other	-2.805	0.0306
SERPINA3	serpin family A member 3	extracellular space	other	-2.803	0.0397
Gm2962	ubiquinol-cytochrome c reductase binding protein pseudogene	other	other	-2.791	0.0137
Gm10710	predicted gene 10710	other	other	-2.789	0.0335
Gm15937	heat shock protein 90, alpha (cytosolic), class A member 1 pseudogene	other	other	-2.774	0.0222
Gm20621	predicted gene 20621	other	other	-2.767	0.0483

Table 3 Part 2: continued

Gm14776	nucleophosmin 1 pseudogene	other	other	-2.734	0.0298
E030026E10Rik	RIKEN cDNA E030026E10 gene	other	other	-2.643	0.041
mir-10	microRNA 100	other	microRNA	-2.639	0.0432
CPNE9	copine family member 9	extracellular space	other	-2.629	0.0309
Gm14239	carnitine deficiency-associated gene expressed in ventricle 3 pseudogene	other	other	-2.612	0.0488
B230398E01Rik	RIKEN cDNA B230398E01 gene	other	other	-2.535	0.0364
WNT4	Wnt family member 4	extracellular space	cytokine	-2.528	0.0316
SNTG1	syntrophin gamma 1	nucleus	other	-2.496	0.0419
Gm7556	aldolase A, fructose-bisphosphate pseudogene	other	other	-2.308	0.0145
6430590A07Rik	RIKEN cDNA 6430590A07 gene	other	other	-2.192	0.0412
DAGLA	diacylglycerol lipase alpha	plasma membrane	enzyme	-2.096	0.0212
HOXA7	homeobox A7	nucleus	transcription regulator	-1.76	0.0417

3.2.2 Altered Genes in Lipid Metabolism Pathways

Dysfunctions of lipid metabolism as well as chronic ongoing inflammation in mesenteric adipose tissue can potentially affect systemic insulin sensitivity. Gene expression of Interleukin 1 beta (IL1B) in mesenteric WAT from male offspring of HFD-fed sires is significantly higher (4.6 fold) in the HFDO compared with the LFDO at 12 months of age when IRI is increased (Table 3). This suggests that chronic inflammation in mesenteric adipose tissue is contributing to the IR. Concomitantly, ALOX15 (arachidonate 15-lipoxygenase), a suppressor of inflammation, is significantly decreased (5.5 fold) in HFDO compared to LFDO (Table 3). Rdh16 (retinol dehydrogenase) is an enzyme that converts all-trans retinol to retinal and can be down-regulated by insulin signaling (138). The observed 3.8-fold increase in Rdh16 in HFDO may be a result of blunted insulin signaling in the insulin resistant HFDO group. Increased Rdh16 will result in decreased adiposity and this may be a compensatory mechanism to prevent further IR (139). On the other hand, DAGLA (diacylglycerol lipase) is decreased by 2-fold in HFDO compared to LFDO, potentially leading to increased levels of DAG. Interestingly, increases in DAG have been implicated in IR, suggesting that its down-regulation may contribute to the IR observed in the HFDO mice (140).

There is decreased differentiation from precursor cells to adipose cells in insulin resistant individuals (141). A number of DEGs related to lipogenesis are also found in the present study. FAM3B, an insulin resistant related cytokine, is elevated in HFDO group compared to LFDO. WNT4 is down regulated by 2.6-fold in the HFDO group. Interestingly, there were several altered miRs in mesenteric adipose tissue of HFDO mice. Certain miRs expressed by adipose tissue that regulate tissue inflammation and insulin sensitivity have been reported by others to be altered in HFD-fed male mice (142). In this study, miR-181 is down regulated by 3.3 fold in HFDO group, and miR-100 is down regulated by 2.6 fold in HFDO group, and miR-155 is down regulated by 3.2 fold (Figure 10).

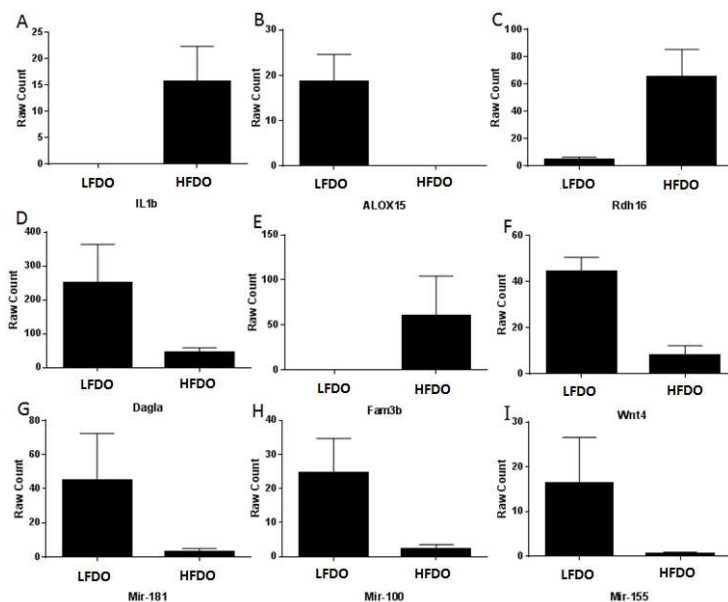


Figure 10. Raw counts of differentially expressed genes. A. IL1b (Interleukin 1 beta); B. ALOX15 (Arachidonate 15-Lipoxygenase); C. Rdh16 (Retinol Dehydrogenase 16); D. Dagla (diacylglycerol lipase alpha ()); E. Fam3b (Family With Sequence Similarity 3 Member B); F. Wnt4 (Wnt Family Member 4); G. mir-181; H. mir-100; I. mir-155.

3.2.3 Ingenuity Pathway Analysis (IPA) of Gene Expression

To identify affected pathways, IPA was performed on these data. The major IPA categories include "Diseases and Disorders, Molecular and Cellular Functions, Physiological System Development and Function, Tox (Toxicology) List, Top Canonical Pathways, and Gene interaction Networks". Based upon the DEGs identified, 192 genes were submitted to the Ingenuity Knowledge Base for functional annotation, mapping genes into canonical pathways and discovering the networks of gene interaction. Of these, IPA recognized 138 genes. As shown in Table 4, the subcategories which showed the major relevant biological process in mesenteric fat include endocrine system development and function, lipid metabolism, cell morphology and cellular development. Note that some genes are represented in more than one pathway.

Table 4. Ingenuity Pathway Analysis

Diseases and Disorders	P-value	Up or down-regulated genes
Dermatological Diseases and Conditions	4.18E-02 - 5.57E-05	5
Developmental Disorder	4.63E-02 - 5.47E-05	5
Organismal Injury and Abnormalities	4.63E-02 - 5.47E-05	25
Neurological Disease	4.63E-02 - 3.58E-03	14
Cancer	4.18E-02 - 3.97E-03	12
Molecular and Cellular Functions	P- value range	Up or down-regulated genes
Cellular Development	4.63E-02 - 1.32 E-04	20
Cellular Assembly and Organization	4.63E-02 - 5.45E-04	22
Lipid Metabolism	4.63E-02 - 6.06E-04	13
Small Molecule Biochemistry	4.63E-02 - 6.07E-04	18
Cell morphology	4.63E-02 - 1.18E-03	17
Physiological System Development and Function	P- value range	Up or down-regulated genes
Endocrine System Development and Function	4.63E-02 - 1.32E-04	10
Tissue Development	4.91E-02 - 5.45 E-04	26
Cardiovascular System Development and Function	4.63E-02 - 5.99 E-04	8
Organismal Development	4.91E-02 - 5.99 E-04	25
Tissue Morphology	4.63E-02 - 5.99 E-04	20

Table 5. continued

Top Toxicological Functions	P- value range	Up or down-regulated genes
Cardiac dysfunction	3.26E-02 - 3.26E-02	1
Cardiac Fibrosis	3.26E-02 - 3.26E-02	1
Cardiac Dilation	4.10E-02 - 1.20E-01	2
Congenital Heart Anomaly	4.07E-02 - 1.45 E-01	1
Cardiac Enlargement	4.69E-02 - 2.96 E-01	2
Glutathione Depletion In Liver	2.80E-02 - 2.80E-02	1
Liver Degeneration	1.41E-01 - 1.41E-01	1
Liver Regeneration	2.07E-01 - 2.07E-01	1
Liver Steatosis	4.26E-01 - 4.26E-01	2
Liver Proliferation	4.58E-01 - 4.58E-01	1
Glomerular Injury	2.00E-01 - 1.88E-02	3
Renal Damage	2.08E-02 - 5.08E-02	1
Renal Tubule Injury	2.08E-02 - 5.08E-02	1
Renal Fibrosis	2.00E-01 - 6.13E-02	2
Kidney Failure	2.00E-01 - 7.71E-02	2

Table 6. continued

Top Canonical Pathways	P-value	Percentage of Up- and down-regulated genes in a particular pathway
TR/RXR Activation	1.00E-02	3.2% 3/94
Neuroprotective Role of THOP1 In Alzheimer's Disease	1.39E-02	2.8% 3/106
Thyronamine and Iodothyronamine Metabolism	1.41E-02	33.3% 1/3
Thyroid Hormone Metabolism I	1.41E-02	33.3% 1/3
Intrinsic Prothrombin Activation pathway	1.46E-02	5.1% 2/39

In the Diseases and Disorders category, there are five molecules related to dermatological disease and conditions and five to developmental disorders. Another 25 genes, such as matrix metalloproteinase 7 (MMP7), are correlated with organismal injury and abnormalities. Fourteen gene products are identified as related to neurological diseases and 12 are correlated with occurrence of cancer. Some gene products appear in multiple subcategories. For example, F2R like trypsin receptor 1 (F2RL1) and forkhead box c2 (Foxc2) are the most highly overlapping molecules (Table 4).

In the Molecular and Cellular Functions category, 20 genes are involved in cellular development, including several transcription factors such as POU class 1 homeobox 1 (POU1F1), T-box 18 (TBX18), and Ephrin B3 (EFNB3). In addition, 22 genes are correlated to cellular assembly and organization, including OCLN, 13 genes are related to lipid metabolism such as arachidonate 15-lipoxygenase (ALOX15), retinol dehydrogenase 16 (all-trans) (Rdh16), and diacylglycerol lipase alpha (DAGLA), 18 gene products are involved in small molecule biochemistry and 17 in cell morphology. ALOX15 and Rdh 16 are the molecules most frequently involved in multiple subcategories (Table 4).

In the Physiological System Development and Function category, 10 gene products are related to endocrine system development and function, 26 to tissue

development, 8 to cardiovascular system development and function, and 25 to organismal development.

In the Top Toxicological Functions category, 7 gene products related to cardiotoxicity are reported linked to cardiac dysfunction, cardiac fibrosis, cardiac dilation, congenital heart anomalies and cardiac enlargement. Six gene products are related to hepatotoxicities, such as glutathione depletion in liver, liver degeneration, liver regeneration, liver steatosis and liver proliferation. Nine gene products are found to be related to nephrotoxicity including glomerular injury, renal damage, renal tubule injury, renal fibrosis and kidney failure. The organ injury information suggests that abnormalities of adipose tissue gene expression have tremendous metabolic effects on other organs. FOXC2, F2RL1 and RNA-binding protein Musashi homolog 1 (MSI1) are commonly shared in multiple subcategories (Table 4).

Among Top Canonical pathways, five were identified as having members of our cohort of 138 genes. Three genes were enriched in the thyroid hormone receptor/retinoic acid receptor (TR/RXR) activation pathway, 3 genes were enriched in the pathway for neuroprotective role of thimet oligopeptidase 1 (THOP1), which degrades beta-amyloid precursor in Alzheimer's disease. They are iodothyronine deiodinase 1 (DIO1), enolase 1 (ENO1) and thyroid stimulating hormone subunit beta (TSH β). DIO1 is also involved in thyronamine and iodothyronamine metabolism and thyroid hormone metabolism I

pathways. Two genes, kallikrein related peptidase 3 (KLK3) and Serpincl, were found in the intrinsic prothrombin activation pathway (Table 4).

As shown in Figures 11 through 14, several networks have been identified by IPA which represent different aspects of biological processes in adipose tissue. FOCUS molecules are those which are up-regulated, shown in red, or downregulated, shown in green, and SCORE can be defined as the magnitude of the sum of the effects of the changes in the FOCUS molecules reflecting both total number of affected genes and the magnitude of change for each. First, some differentially expressed genes found in mesenteric adipose tissue of HFDO mice form a network encompassing lipid metabolism, inflammatory processes, molecular transport and small molecule biochemistry (Figure 11). Other differentially expressed genes form a network related to cell death and survival, amino acid metabolism and cellular function and maintenance (Figure 12). Some molecules form a third network related to organismal injury and abnormalities, and renal damage (Figure 13). Finally, some trans-membrane molecules form a network related to endocrine function, molecular transport and lipid synthesis enzymes, which may indicate that multiple interactions of hormones are affected (Figure 14). For example this pathway includes several enzymes involved in steroid synthesis and interconversion such as aromatase (CYP19A1) and 17 α -hydroxylase (CYP17A1).

Pathway involved	Focus molecules	Score
Lipid metabolism, Molecular transport, Small molecule Biochemistry	20	38

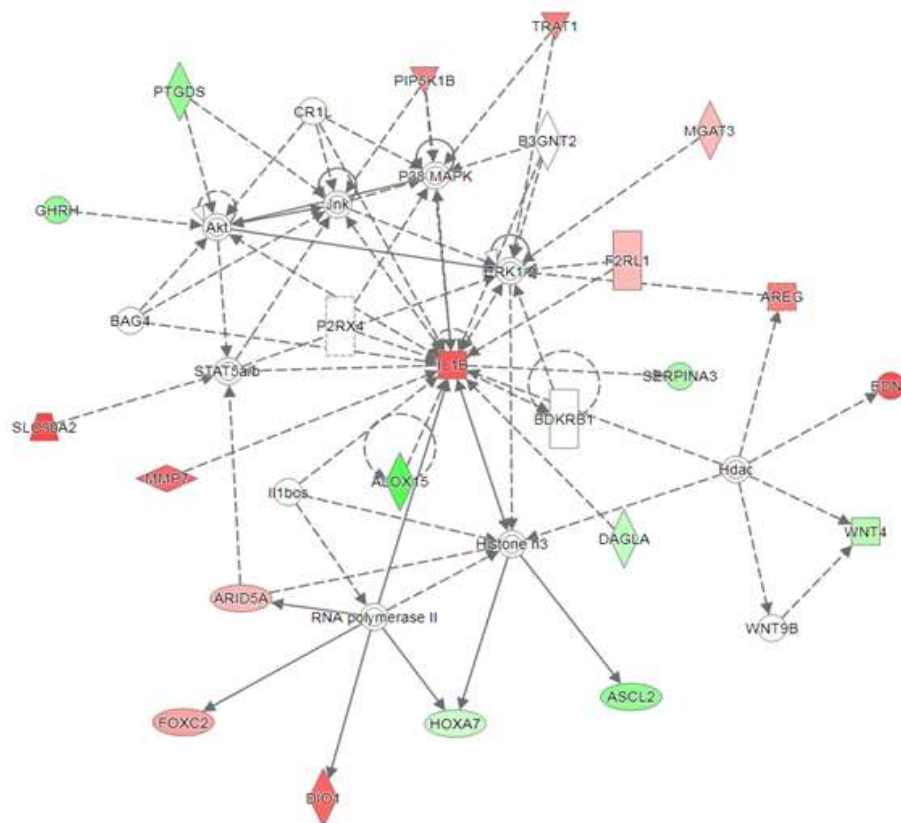


Figure 11. Network of lipid metabolism, molecular transport and small molecule biochemistry. Red color: up-regulated genes. Green color: Down-regulated genes. The darker the color, the more fold changes in the molecule.

Pathway involved	Focus molecules	Score
cell death and survival, amino acid metabolism and cellular function and maintenance	16	28

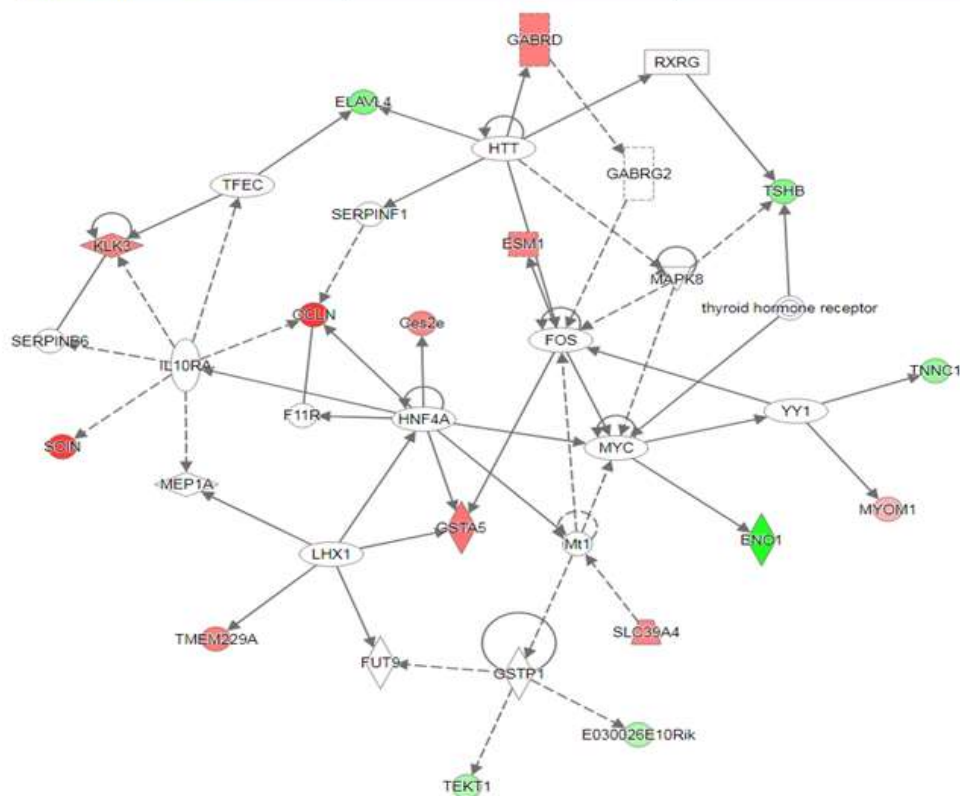


Figure 12. Network of cell death and survival, amino acid metabolism and cellular function and maintenance. Red color: up-regulated genes. Green color: Down-regulated genes. The darker the color, the more fold changes the molecule.

Pathway involved	Focus molecules	Score
organismal injury and abnormalities and renal damage	12	19

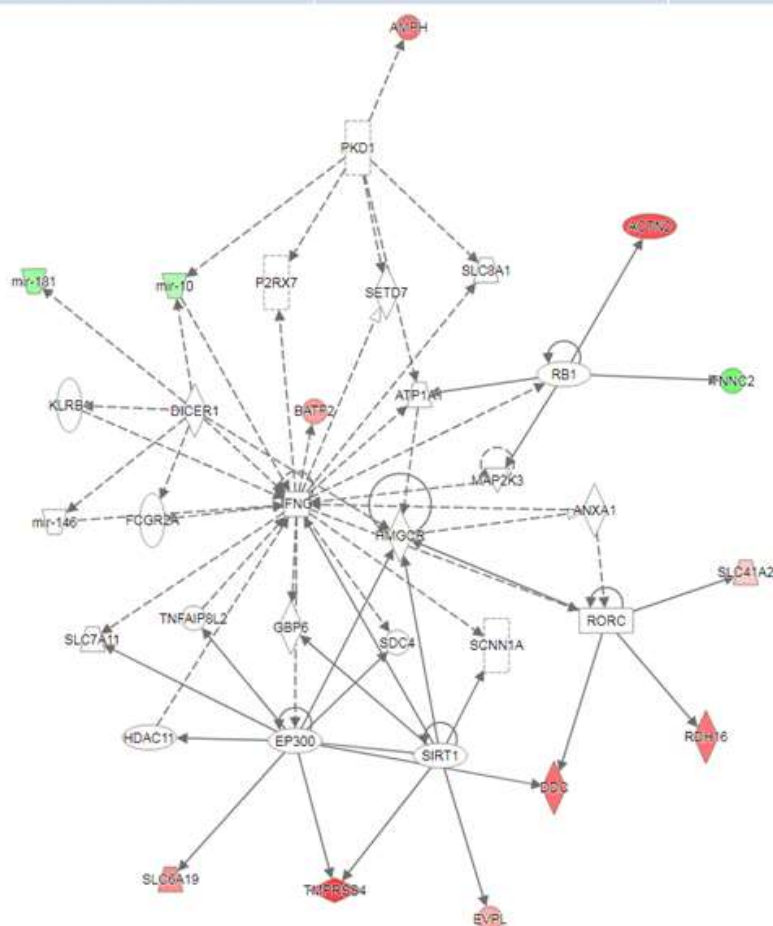


Figure 13. Network of organismal injury and abnormalities and renal damage. Red color: up-regulated genes. Green color: Down-regulated genes. The darker the color, the more fold change in the molecule.

Pathway involved	Focus molecules	Score
endocrine system development and function, molecular transport and small molecule biochemistry	9	13

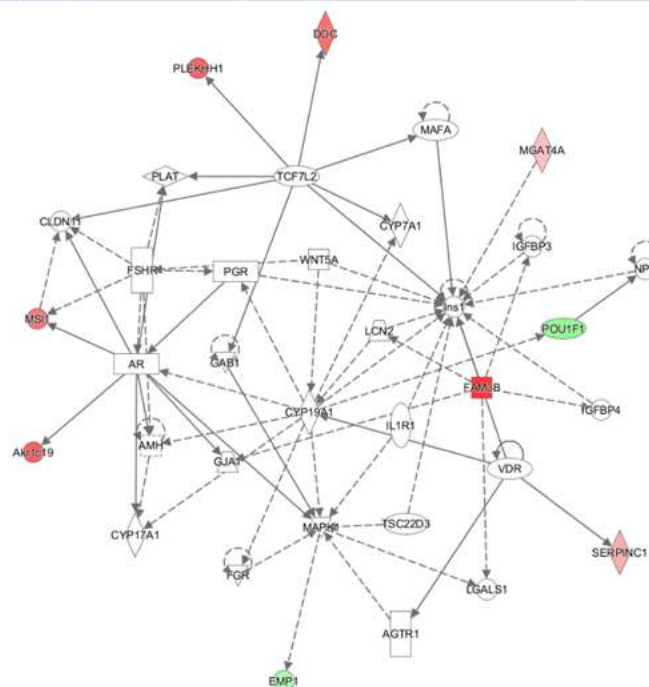


Figure 14. Network of endocrine system development and function, molecular transport and small molecule biochemistry. Red color: up-regulated genes. Green color: Down-regulated genes. The darker the color, the more fold change in the molecule.

3.2.4 DNA Methylation Analysis of DEGs in Adipose Tissue

When comparing LFDO and HFDO, we found no significant difference in the average percentage of DNA methylation in the CpG islands in the promoter regions of 7 DEGs related to lipid metabolism and endocrine function (MGAT3, PIP5K1b, WNT, AREG, Dagla, Efnb, ENO1b) (Figures 15-21). There are data from only 4 mice for gene Efnb because data of the other 2 available mice did not pass quality control (Figure 19).

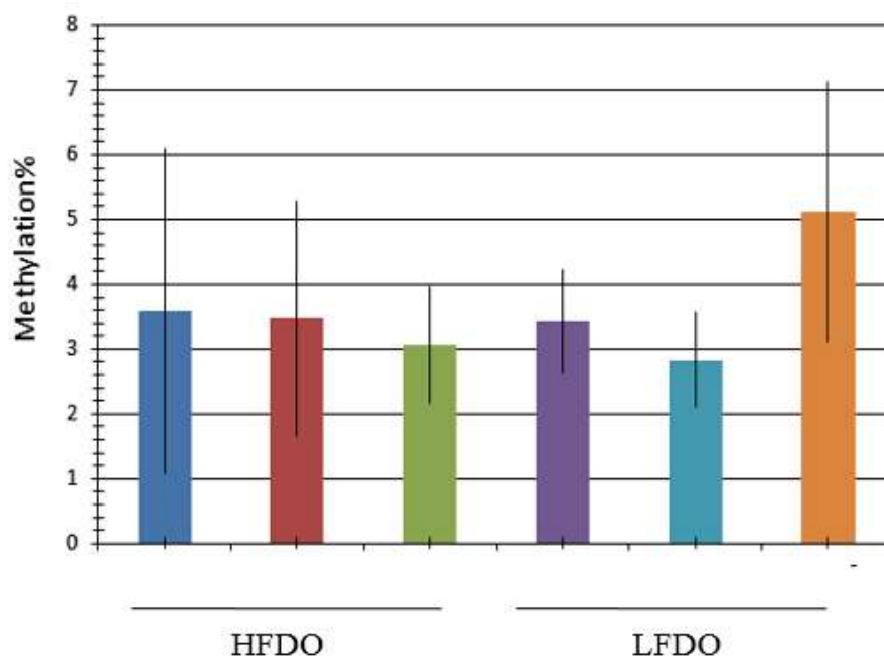


Figure 15. MGAT3 Promoter CpG Island Methylation Status. Each column represents the average methylation percentage of multiple CpG islands (n=10) in the amplified PCR products from one mouse.

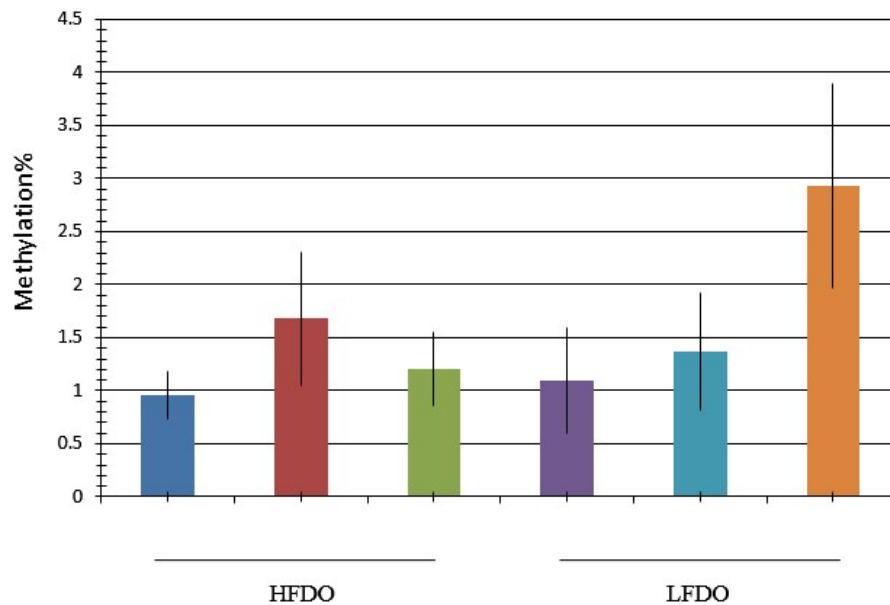


Figure 16. PIP5K1b Promoter CpG Island Methylation Status. Each column represents the average methylation percentage of multiple CpG islands (n=7) in the amplified PCR products from one mouse.

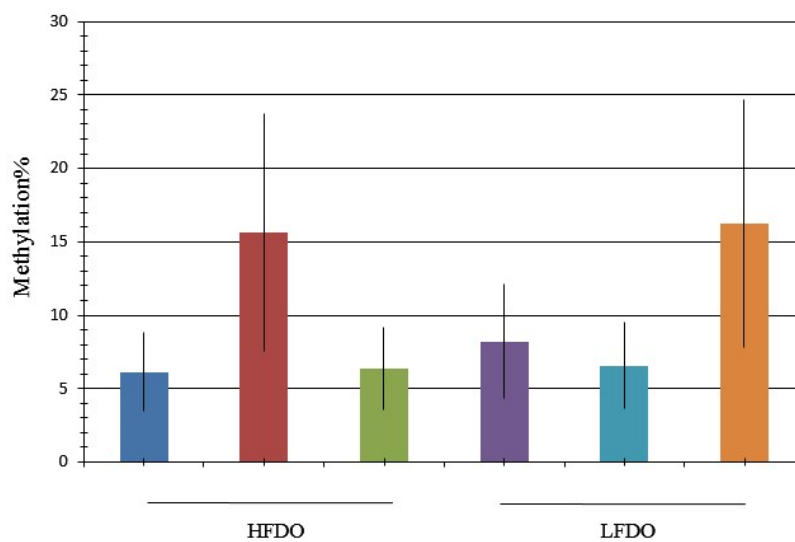


Figure 17. WNT4 Promoter CpG Island Methylation Status. Each column represents the average methylation percentage of multiple CpG islands (n=7) in the amplified PCR products from one mouse.

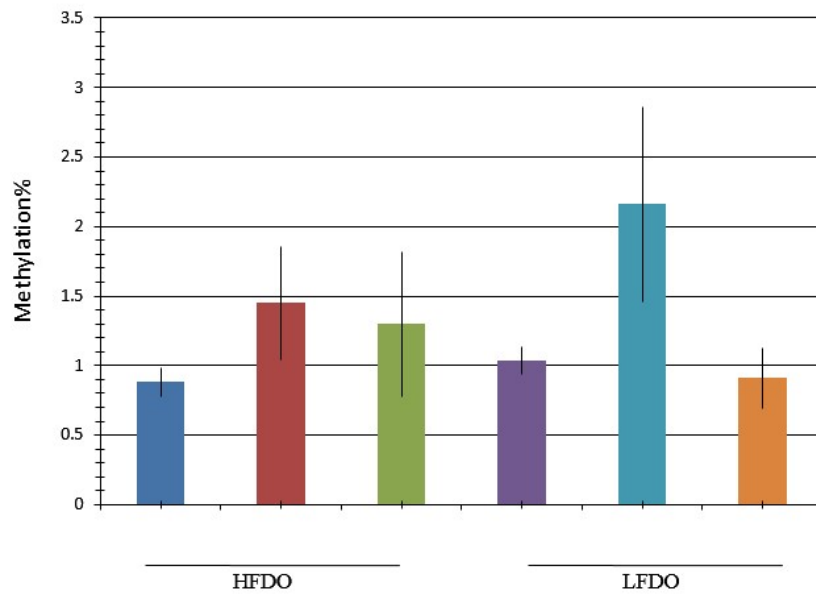


Figure 18. AREG Promoter CpG Island Methylation Status. Each column represents the average methylation percentage of multiple CpG islands (n=7) in the amplified PCR products from one mouse.

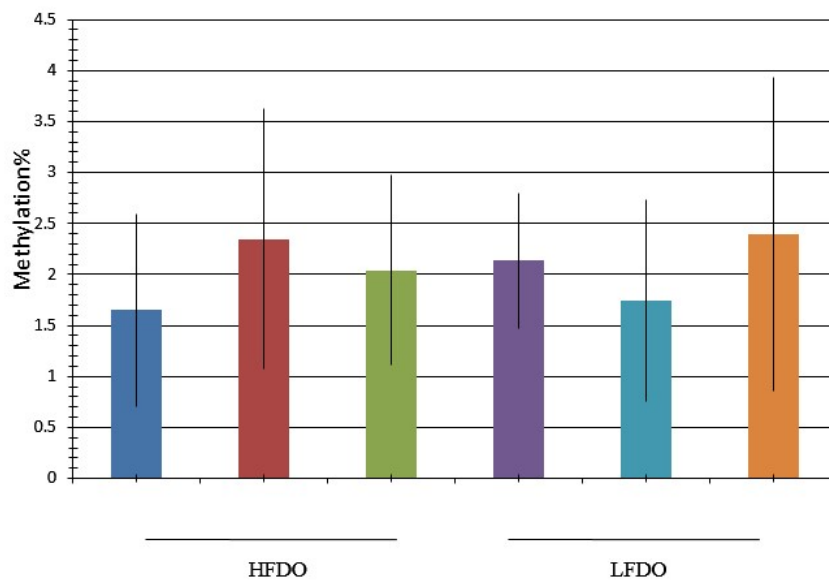


Figure 19. DAGLA Promoter CpG Island Methylation Status. Each column represents the average methylation percentage of multiple CpG islands (n=10) in the amplified PCR products from one mouse.

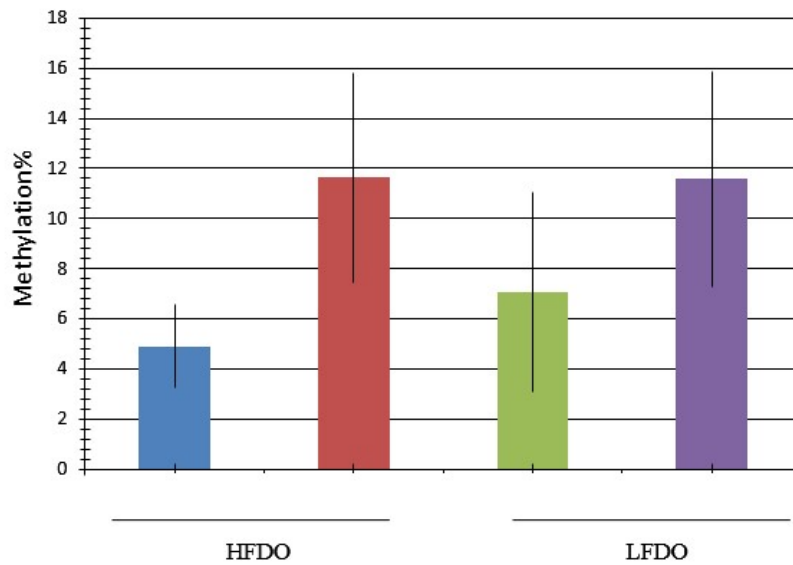


Figure 20. Efnb Promoter CpG Island Methylation Status. Each column represents the average methylation percentage of multiple CpG islands (n=10) in the amplified PCR products from one mouse.

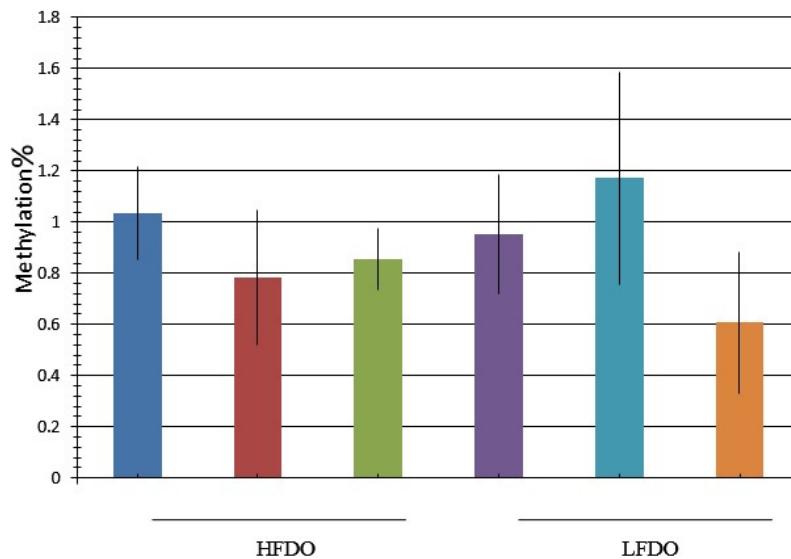


Figure 21. ENO1b Promoter CpG Island Methylation Status. Each column represents the average methylation percentage of multiple CpG islands (n=8) in the amplified PCR products from one mouse.

CHAPTER 4: DISCUSSION

4.1 Role of Gastrocnemius Muscle GLUT4 in Insulin Resistance

This study is the first to observe IR in male offspring in the setting of preconception HFD-induced paternal obesity in mice. Recently it was shown that insulin signaling is enhanced in young (1.5 month) offspring of HFD-fed fathers, but this effect is reversed as the animals age (143). This finding is in agreement with the observed decrease in insulin sensitivity in 12-month middle aged mice (Figure 4C).

The results from this study also show a sex difference in expression of GLUT4, with approximately 50% higher mean level in LFDO females and 65% higher mean level in HFDO females, compared to their male counterparts (Figure 6B). In agreement with the current results, higher levels of total GLUT4 in skeletal muscle in female mice versus males have been observed by others (122). This may be due to estrogen up-regulation of GLUT4 expression, as Barros et al. found that expression of GLUT4 is significantly reduced in skeletal muscle of estrogen-receptor (ER) α (-/-) knockout mice (144). There is also a marked reduction of GLUT4 at plasma membrane in these mice. GLUT4 is also altered by maternal diet. Zheng et al. studied the effect of maternal protein restriction on gastrocnemius muscle GLUT4 expression. The low protein female offspring demonstrated higher levels of GLUT4 than control diet offspring (145).

Even though HFDO exhibit increased IR at 12 months of age, when the 12 month time point is considered alone, total GLUT4 expression in male offspring gastrocnemius muscle was not significantly different between LFDO and HFDO (Figure 6). Nor was plasma membrane GLUT4 expression significantly different between LFDO and HFDO (Figure 7A). When data from all males of each diet group are analyzed together, total GLUT4 does not show a difference between diet groups (Figure 6). This suggests that GLUT4 is a stably expressed protein in the early stage of IR and that initially its synthesis is not affected by an individual's own insulin sensitivity or metabolic status of sires. Shan et al. found that neither GLUT4 mRNA nor protein levels of total GLUT4 in muscle tissue of cirrhosis patients with IR differed from those in healthy controls (146). This is in agreement with the results of this study. As discovered next, there is another mechanism that is responsible for the observed partially compensated IR.

It was next hypothesized that the trafficking of GLUT4 is affected in the IR male offspring. A muscle tissue fractionation protocol was developed to enable measurement of GLUT4 in functionally relevant subcellular compartments, including plasma membrane, cytosol and GSV using immunoblot analysis. Interestingly, HFDO males of each age group have higher GLUT4 expression on the plasma membrane than LFDO males. (Figure 7A). As there are no statistically significant differences in either group with age, age groups were combined and, as shown in Figure 7B, there is a significant

difference between HFDO and LFDO males. Since there is no difference in fasting glucose between LFDO and HFDO (data not shown), this supports the concept of increased glucose uptake under basal state to prevent hyperglycemia. It is concluded that the IR observed in HFDO males is a relatively early stage of IR which is not due to decreased glucose uptake by muscle. Instead, muscle is transferring more GLUT4 to the plasma membrane to prevent overt IR. It has been suggested that group differences in physical activity or brown fat are a cause for some of the observed difference in GLUT4 trafficking. Body composition, swim time, voluntary running and fat depot weights were also measured in all groups of mice (127). An increase in active swim time was seen in HFDO males compared to LFDO males at 6 months. This HFDO group also had an increase in % body fat (127). However by 12 months of age, there were no significant diet group differences in % body fat, brown adipose tissue or physical activity in males. Garvey et al. reported that impaired GLUT4 translocation contributes to IR and type 2 diabetes (147) with decreased amounts of GLUT4 in the plasma membrane. The apparent conflict with the results in this study is most likely due to the early state of metabolic dysfunction in the mice in contrast to patients with severe IR or diabetes who have reached a more advanced stage of IR and now present with malfunction of GLUT4 trafficking in muscle (148).

In the normal basal state, GLUT4 located in cytosol can be as high as 95% of total GLUT4 while GLUT4 located on plasma membrane can be as low as 5% of total cellular GLUT4 (149). Increased insertion of GLUT4 from GSV into the plasma membrane can be initiated by insulin stimulation (150). Cytosol GLUT4 has two pools. The first is the endosomal recycling system which is highly dynamic and responsible for most of GLUT4 endocytosis and exocytosis under basal conditions. At any given time, there is a minimal concentration of GLUT4 in endosomes. The second pool is in the GSV. This pool is more static and contains more than 70% of total cellular GLUT4. Under basal conditions, insertion of GLUT4 into the plasma membrane occurs by circulation between the GSV and plasma membrane (150). In the present study, Rab11, a marker for endosomes, was used to distinguish the dynamic endosomes from the GSV pool. Mean GLUT4 expression in cytosol in HFDO was approximately 50% that in LFDO at 12 months. In the insulin resistant HFDO mice which have an increased value of glucose x insulin (IRI), the GLUT4 relocated to plasma membrane was high enough to make a significant difference in this 5% component of total cellular GLUT4 (Figure 7B). However, this 50% difference, also seen in GSV (Figure 8 C), is not enough to make the same magnitude of difference in the larger 95% component of GLUT4. This reciprocal shift in the location of GLUT4 from one compartment to another is in agreement with there being no difference in total cellular GLUT4 between LFDO and HFDO (Figure 6).

Inheritance of obesity occurs between parents and children and even between grandparents and grandchildren (151, 152). Veena et al. reported that both maternal and paternal obesity are associated with and predictive of childhood adiposity and IR in Asian Indian children (153). HFDO exhibit many different phenotypic characteristics when compared to LFDO. Multiple molecular mechanisms have been discovered by which paternal diet can influence the metabolic profile of offspring. In this study, different apparent strategies in male versus female offspring of HFD-fed fathers were observed. This is consistent with an epigenetic mode of transmission, not a genetic one.

Non-genomic inheritance through gametes and carriers of epigenetic information such as DNA methylation, chromatin proteins and non-coding RNAs has been demonstrated in a number of studies (154). For example, paternal HFD modulates histone composition on genes implicated in developmental processes in paternal spermatozoa and significantly alters the mRNA level of 7 genes in livers of male offspring compared to LFD-sire control mice (155). Epigenetic changes can also be transmitted to the next generation through sperm which exhibit hypo-methylation of specific genes (156). Carone et al. reported that paternal low protein diet can induce upregulation of lipid biosynthesis genes in livers of offspring mice; differentially methylated loci, identified by bisulfite sequencing, resulted in altered levels of specific fatty acids and cholesterol (157). Sperm miRs and tRNA-derived small RNAs (tsRNAs)

have also been found to mediate diet induced inheritance of metabolic disorders from fathers (158, 159). Fullston et al. found that paternal obesity causes metabolic abnormalities in two subsequent generations by altering miRs in testis and sperm (100, 160). Metabolic disturbances in male offspring sired by HFD fathers are exacerbated by feeding the offspring a HFD. However, paternal diet has a greater influence than offspring diet on serum glucose levels in offspring (161). The molecular mechanisms behind the effects found here on GLUT4 localization in males and total GLUT4 in females versus males remain to be determined.

In conclusion, it is shown that male offspring of obese HFD-fed fathers develop increased IR by 12 months of age. Expression of GLUT4 on plasma membrane of these HFDO males is significantly higher than in LFDO males. This suggests a compensatory increase in muscle tissue glucose uptake in regular low-fat chow-fed male offspring of HFD-fed sires. In contrast, females do not develop IR, possibly due to preexisting higher levels of GLUT4, a different mechanism, but one which might also mediate increased uptake of glucose into muscle with the additional increase of 22% in HFDO seen here. Some attributes of HFD-sire offspring mirror those seen in the obese parent, while others appear to be an attempt to protect the offspring from the harmful consequences of eating a similar diet. Once determined the mechanism behind the upregulation of GLUT4 in

skeletal muscle will be a potential therapeutic target for patients with IR or type 2 diabetes.

4.2 Adipose Tissue and Insulin Resistance

The possible mechanisms that initiate IR include abnormal glucose metabolism in liver and increased inflammation in muscle and adipose tissue caused by certain adipokines (162, 163). Consequently, how mesenteric adipose tissue contributes to IR of male offspring of obese fathers was explored next. Adipose tissue can release adipokines and FFA which inhibit insulin signaling and thus increase IR (164). Hepatic IR can also be caused by aberrant production of certain adipokines, initiating chronic inflammation and inhibiting insulin signaling at the levels of insulin receptor and insulin receptor substrate levels. As a result, suppression of hepatic gluconeogenesis is impaired and hyperglycemia occurs (165). Increased levels of IL1B along with pro-inflammatory adipokines TNF- α and IL-6 indicate chronic inflammation status of obese individuals and are correlated with IR (104, 166, 167). In addition, Rakotoarivelo et al. found that IL1B was significantly elevated in the visceral adipose tissues of obese patients (168). The higher IL1B levels in mesenteric adipose tissue from HFDO mice in the present study may thus indicate the occurrence of chronic inflammation there as well, which is contributing to the observed IR.

On the other hand, ALOX15 is a factor that can function as an inhibitor of inflammation (169). It is down regulated in the HFDO mice which could thus facilitate the progression of chronic inflammation. ALOX15 may also be responsible for non-inflammatory removal of adipocytes during adipose tissue remodeling. It is up-regulated in WAT macrophages when the apoptotic adipocyte death is increased (170). FAM3b (The Family with Sequence Similarity 3), was initially identified as a pancreatic-derived factor that was shown to induce islet apoptosis in endocrine pancreas via the caspase-3-dependent pathway (171). It has since been recognized that FAM3b is a member of a widely expressed family of cytokines that also function as inducers of IR and lipogenesis (172, 173). FAM3b was found to be elevated in the HFDO mice, suggesting it may also be contributing to the insulin resistant state. WNT4 and WNT5a are positive regulators of adipogenesis (174). Inhibition of WNT4 and WNT5a has been shown to result in decreased expression of adipogenesis-related genes and reduced accumulation of triacylglycerol (174). WNT4 is specifically secreted by skeletal muscle and adipose tissue during the development of IR and plays an important role in cross-talk between insulin-resistant tissues and pancreatic beta cells. Kozinski et al. found that WNT4 production in WAT was decreased during the pre-diabetic state to promote insulin secretion (175). However in patients with fully developed diabetes, the expression profile of Wnt4 in adipose tissue and muscle cells and blood plasma levels of this protein were

opposite to the pre-diabetic state, thus favoring the downregulation of Wnt signaling in beta cells and resulting in dysfunctional pancreatic islets. Interestingly, mesenteric adipose tissue WNT4 is down regulated in the HFDO group consistent with these mice having not yet reached a full developed diabetic state.

DAGLA, an enzyme involved in eicosanoid signaling correlated with adipogenesis, is down regulated in the HFDO group (Table 4). This is in accordance with the results of other colleagues. Resnyk et al., using RNA-seq analysis, found that genetically fat chickens show insulin insensitivity and have lower DAGLA expression in abdominal adipose tissue when compared to lean chickens (176). They also exhibit over-expression of numerous adipogenic and lipogenic genes suggesting that in situ lipogenesis increases in chickens with IR. It is possible that this decrease in DAGLA also contributes to the increased body fat and WAT mass in the HFDO mice.

Finally, alterations in expression of several miRs, mir-181, mir-155 and mir-100 in the mesenteric adipose tissue of HFDO mice were identified (Figure 10). miR-181 is recognized as an important modulator of neuronal function and development of lymphocytes. Recently, Chu et al. found that mir-181 also has an important role in regulation of lipid metabolism. miR-181 inhibits lipid accumulation, targeting isocitrate dehydrogenase (IDH1), which results in decreased expression of genes involved in lipid synthesis and increased expression of genes involved in β -oxidation. (177). miR-181 is

down regulated in the HFDO mice, which could facilitate mesenteric adipose tissue accumulation (Figure 10). A known inhibitor of adipogenesis, miR-155, is also down regulated in the HFDO mice; this would also favor lipid accumulation (Figure 10). Finally, mir-100 has been found to be down regulated during adipogenesis in humans (81). miR-100 was down regulated in the HFDO mice (Figure 10). In summary, downregulation of three miRs in mesenteric adipose tissue of HFDO may promote increased fat accumulation by decreasing the normal inhibition of adipogenesis necessary to maintain metabolic balance.

Although differences in promoter methylation were not detected in the present study, several alterations in miRs were found. Other studies have identified dysregulation of miRs in sperm and placenta associated with parental obesity. Carreras-Badosa et al. reported that several miRNAs including mir-100 were decreased in placentas and were associated with maternal metabolic status and predictors of low birth weight (178). Sperm miR content has been shown to be altered in obese mice and metabolic abnormalities can be transmitted to F2 generation (100). In fact, alterations in a miR can subsequently alter the promoter methylation of multiple genes leading to widespread changes in offspring metabolism. The altered miR profile of male offspring can be rescued by pre-conception exercise by obese fathers (179). Paternal obesity can also

cause increased oxidative stress in sperm leading to DNA damage and ineffective DNA repair; this may contribute to metabolic disturbances in offspring (180).

Network analysis showed that Alox 15, as an inhibitor of inflammation can regulate IL1B (Figure 11) which is consistent with the RNA sequencing result that Alox 15 is down-regulated while IL1B is up-regulated (Table 4). Network of cell death and survival and cellular function and maintenance suggests there might be dysfunction of adipogenesis and apoptosis of adipocytes (Figure 12). Network of organismal injury and real damage has relatively low molecule interactions (Figure 13). This suggests dysfunction of adipose tissue can negatively affect other organs such as kidney, although such effect may be weak. This is interesting in light of the finding that children with severe obesity have elevated biomarkers for early renal injury and increased prevalence of early renal disease (86). Network related to endocrine system showed there are interactions between synthesis pathway of one hormone and signaling pathways of another hormone (Figure 14).

In summary, this study demonstrated for the first time that (1) male offspring of HFD-induced obese sires develop IR in middle age (12 months), (2) this IR may be compensated by alterations in the subcellular distribution of GLUT4, one of two major glucose transporters in muscle, (3) gastrocnemius GSV can be isolated by the subcellular fractionation protocol described here, allowing for GSV GLUT4 quantification by

immunoblotting, (4) HFDO males have increased translocation of GLUT4 to the plasma membrane, where the transport function takes place, when compared to LFDO males. (5) mesenteric adipose tissue of male offspring of HFD-induced obese sires differentially expresses 192 genes; 113 genes are upregulated and 79 are downregulated, (6) the products of these genes are both mRNAs and miRs, (7) IPA places the mRNAs in networks that involve cell death and survival, lipid metabolism, molecular transport, and endocrine system interactions, that include insulin (8) three miRs that inhibit lipid accumulation are downregulated in HFDO mesenteric adipose tissue, favoring adipogenesis. This study also confirmed the previous finding that females have higher levels of total muscle GLUT4 than males.

REFERENCES

1. Flegal KM, Carroll MD, Ogden CL, Curtin LR. Prevalence and trends in obesity among US adults, 1999-2008. *Jama*. 2010 Jan 20;303(3):235-41. PubMed PMID: 20071471.
2. Ogden CL, Carroll MD, Fryar CD, Flegal KM. Prevalence of Obesity Among Adults and Youth: United States, 2011-2014. *NCHS data brief*. 2015 Nov(219):1-8. PubMed PMID: 26633046.
3. Skinner AC, Ravanbakht SN, Skelton JA, Perrin EM, Armstrong SC. Prevalence of Obesity and Severe Obesity in US Children, 1999-2016. *Pediatrics*. 2018 Feb 26. PubMed PMID: 29483202.
4. Kamijo K, Pontifex MB, Khan NA, Raine LB, Scudder MR, Drollette ES, et al. The negative association of childhood obesity to cognitive control of action monitoring. *Cerebral cortex*. 2014 Mar;24(3):654-62. PubMed PMID: 23146965.
5. Sewell MF, Huston-Presley L, Super DM, Catalano P. Increased neonatal fat mass, not lean body mass, is associated with maternal obesity. *American journal of obstetrics and gynecology*. 2006 Oct;195(4):1100-3. PubMed PMID: 16875645.
6. Li S, Zhao JH, Luan J, Langenberg C, Luben RN, Khaw KT, et al. Genetic predisposition to obesity leads to increased risk of type 2 diabetes. *Diabetologia*. 2011 Apr;54(4):776-82. PubMed PMID: 21267540.
7. Zimmet PZ, Magliano DJ, Herman WH, Shaw JE. Diabetes: a 21st century challenge. *The Lancet Diabetes & Endocrinology*. 2014;2(1):56-64. PMID: 24622669.
8. Hillier TA, Pedula KL. Characteristics of an adult population with newly diagnosed type 2 diabetes: the relation of obesity and age of onset. *Diabetes care*. 2001 Sep;24(9):1522-7. PubMed PMID: 11522693.

9. Ling C, Del Guerra S, Lupi R, Ronn T, Granhall C, Luthman H, et al. Epigenetic regulation of PPARGC1A in human type 2 diabetic islets and effect on insulin secretion. *Diabetologia*. 2008 Apr;51(4):615-22. PubMed PMID: 18270681.
10. Leiter EH, Coleman DL, Hummel KP. The influence of genetic background on the expression of mutations at the diabetes locus in the mouse. III. Effect of H-2 haplotype and sex. *Diabetes*. 1981 Dec;30(12):1029-34. PubMed PMID: 7030828.
11. Tremblay MS, Katzmarzyk PT, Willms JD. Temporal trends in overweight and obesity in Canada, 1981-1996. *International journal of obesity and related metabolic disorders : journal of the International Association for the Study of Obesity*. 2002 Apr;26(4):538-43. PubMed PMID: 12075581.
12. Bonora E, Formentini G, Calcaterra F, Lombardi S, Marini F, Zenari L, et al. HOMA-estimated insulin resistance is an independent predictor of cardiovascular disease in type 2 diabetic subjects: prospective data from the Verona Diabetes Complications Study. *Diabetes care*. 2002 Jul;25(7):1135-41. PubMed PMID: 12087010.
13. Rull A, Camps J, Alonso-Villaverde C, Joven J. Insulin resistance, inflammation, and obesity: role of monocyte chemoattractant protein-1 (or CCL2) in the regulation of metabolism. *Mediators of inflammation*. 2010;2010. PubMed PMID: 20936118.
14. Weisberg SP, McCann D, Desai M, Rosenbaum M, Leibel RL, Ferrante AW, Jr. Obesity is associated with macrophage accumulation in adipose tissue. *The Journal of clinical investigation*. 2003 Dec;112(12):1796-808. PubMed PMID: 14679176.
15. Xu H, Barnes GT, Yang Q, Tan G, Yang D, Chou CJ, et al. Chronic inflammation in fat plays a crucial role in the development of obesity-related insulin resistance. *The Journal of clinical investigation*. 2003 Dec;112(12):1821-30. PubMed PMID: 14679177.
16. Gordon S, Taylor PR. Monocyte and macrophage heterogeneity. *Nature reviews Immunology*. 2005 Dec;5(12):953-64. PubMed PMID: 16322748.

17. Mantovani A, Sica A, Sozzani S, Allavena P, Vecchi A, Locati M. The chemokine system in diverse forms of macrophage activation and polarization. *Trends in immunology*. 2004 Dec;25(12):677-86. PubMed PMID: 15530839.
18. Lumeng CN, Bodzin JL, Saltiel AR. Obesity induces a phenotypic switch in adipose tissue macrophage polarization. *The Journal of clinical investigation*. 2007 Jan;117(1):175-84. PubMed PMID: 17200717.
19. Lumeng CN, DelProposto JB, Westcott DJ, Saltiel AR. Phenotypic switching of adipose tissue macrophages with obesity is generated by spatiotemporal differences in macrophage subtypes. *Diabetes*. 2008 Dec;57(12):3239-46. PubMed PMID: 18829989.
20. Canello R, Henegar C, Viguerie N, Taleb S, Poitou C, Rouault C, et al. Reduction of macrophage infiltration and chemoattractant gene expression changes in white adipose tissue of morbidly obese subjects after surgery-induced weight loss. *Diabetes*. 2005 Aug;54(8):2277-86. PubMed PMID: 16046292.
21. Rausch ME, Weisberg S, Vardhana P, Tortoriello DV. Obesity in C57BL/6J mice is characterized by adipose tissue hypoxia and cytotoxic T-cell infiltration. *International journal of obesity*. 2008 Mar;32(3):451-63. PubMed PMID: 17895881.
22. Yu X, Druz S, Graves DT, Zhang L, Antoniadis HN, Hollander W, et al. Elevated expression of monocyte chemoattractant protein 1 by vascular smooth muscle cells in hypercholesterolemic primates. *Proceedings of the National Academy of Sciences of the United States of America*. 1992 Aug 1;89(15):6953-7. PubMed PMID: 1379728.
23. Gu L, Okada Y, Clinton SK, Gerard C, Sukhova GK, Libby P, et al. Absence of monocyte chemoattractant protein-1 reduces atherosclerosis in low density lipoprotein receptor-deficient mice. *Molecular cell*. 1998 Aug;2(2):275-81. PubMed PMID: 9734366.
24. Vila-del Sol V, Punzon C, Fresno M. IFN-gamma-induced TNF-alpha expression is regulated by interferon regulatory factors 1 and 8 in mouse macrophages. *Journal of immunology*. 2008 Oct 1;181(7):4461-70. PubMed PMID: 18802049.

25. Shanik MH, Xu Y, Skrha J, Dankner R, Zick Y, Roth J. Insulin resistance and hyperinsulinemia: is hyperinsulinemia the cart or the horse? *Diabetes care*. 2008 Feb;31 Suppl 2:S262-8. PubMed PMID: 18227495.
26. Hotamisligil GS, Shargill NS, Spiegelman BM. Adipose expression of tumor necrosis factor- α : direct role in obesity-linked insulin resistance. *Science*. 1993 Jan 1;259(5091):87-91. PubMed PMID: 7678183.
27. Fried SK, Bunkin DA, Greenberg AS. Omental and subcutaneous adipose tissues of obese subjects release interleukin-6: depot difference and regulation by glucocorticoid. *The Journal of clinical endocrinology and metabolism*. 1998 Mar;83(3):847-50. PubMed PMID: 9506738.
28. Bastard JP, Maachi M, Van Nhieu JT, Jardel C, Bruckert E, Grimaldi A, et al. Adipose tissue IL-6 content correlates with resistance to insulin activation of glucose uptake both in vivo and in vitro. *The Journal of clinical endocrinology and metabolism*. 2002 May;87(5):2084-9. PubMed PMID: 11994345.
29. Ihle JN, Witthuhn BA, Quelle FW, Yamamoto K, Silvennoinen O. Signaling through the hematopoietic cytokine receptors. *Annual review of immunology*. 1995;13:369-98. PubMed PMID: 7612228.
30. Stepan CM, Bailey ST, Bhat S, Brown EJ, Banerjee RR, Wright CM, et al. The hormone resistin links obesity to diabetes. *Nature*. 2001 Jan 18;409(6818):307-12. PubMed PMID: 11201732.
31. Makki K, Froguel P, Wolowczuk I. Adipose tissue in obesity-related inflammation and insulin resistance: cells, cytokines, and chemokines. *ISRN inflammation*. 2013 Dec 22;2013:139239. PubMed PMID: 24455420.
32. El-Shal AS, Pasha HF, Rashad NM. Association of resistin gene polymorphisms with insulin resistance in Egyptian obese patients. *Gene*. 2013 Feb 15;515(1):233-8. PubMed PMID: 23178185.

33. Henriksen EJ, Dokken BB. Role of glycogen synthase kinase-3 in insulin resistance and type 2 diabetes. *Current drug targets*. 2006 Nov;7(11):1435-41. PubMed PMID: 17100583.
34. Mackenzie RW, Elliott BT. Akt/PKB activation and insulin signaling: a novel insulin signaling pathway in the treatment of type 2 diabetes. *Diabetes, metabolic syndrome and obesity : targets and therapy*. 2014;7:55-64. PubMed PMID: 24611020.
35. White MF. IRS proteins and the common path to diabetes. *American journal of physiology Endocrinology and metabolism*. 2002 Sep;283(3):E413-22. PubMed PMID: 12169433.
36. Whitehead JP, Humphreys P, Krook A, Jackson R, Hayward A, Lewis H, et al. Molecular scanning of the insulin receptor substrate 1 gene in subjects with severe insulin resistance: detection and functional analysis of a naturally occurring mutation in a YMXM motif. *Diabetes*. 1998 May;47(5):837-9. PubMed PMID: 9588458.
37. Yamauchi T, Tobe K, Tamemoto H, Ueki K, Kaburagi Y, Yamamoto-Honda R, et al. Insulin signalling and insulin actions in the muscles and livers of insulin-resistant, insulin receptor substrate 1-deficient mice. *Molecular and cellular biology*. 1996 Jun;16(6):3074-84. PubMed PMID: 8649419.
38. Previs SF, Withers DJ, Ren JM, White MF, Shulman GI. Contrasting effects of IRS-1 versus IRS-2 gene disruption on carbohydrate and lipid metabolism in vivo. *The Journal of biological chemistry*. 2000 Dec 15;275(50):38990-4. PubMed PMID: 10995761.
39. Cheatham B, Vlahos CJ, Cheatham L, Wang L, Blenis J, Kahn CR. Phosphatidylinositol 3-kinase activation is required for insulin stimulation of pp70 S6 kinase, DNA synthesis, and glucose transporter translocation. *Molecular and cellular biology*. 1994 Jul;14(7):4902-11. PubMed PMID: 8007986.
40. Okada T, Kawano Y, Sakakibara T, Hazeki O, Ui M. Essential role of phosphatidylinositol 3-kinase in insulin-induced glucose transport and antilipolysis in rat

adipocytes. Studies with a selective inhibitor wortmannin. *The Journal of biological chemistry*. 1994 Feb 4;269(5):3568-73. PubMed PMID: 8106400.

41. Cho H, Thorvaldsen JL, Chu Q, Feng F, Birnbaum MJ. Akt1/PKBalpha is required for normal growth but dispensable for maintenance of glucose homeostasis in mice. *The Journal of biological chemistry*. 2001 Oct 19;276(42):38349-52. PubMed PMID: 11533044.

42. Cho H, Mu J, Kim JK, Thorvaldsen JL, Chu Q, Crenshaw EB, 3rd, et al. Insulin resistance and a diabetes mellitus-like syndrome in mice lacking the protein kinase Akt2 (PKB beta). *Science*. 2001 Jun 1;292(5522):1728-31. PubMed PMID: 11387480.

43. Summers SA, Kao AW, Kohn AD, Backus GS, Roth RA, Pessin JE, et al. The role of glycogen synthase kinase 3beta in insulin-stimulated glucose metabolism. *The Journal of biological chemistry*. 1999 Jun 18;274(25):17934-40. PubMed PMID: 10364240.

44. Bogardus C, Lillioja S, Stone K, Mott D. Correlation between muscle glycogen synthase activity and in vivo insulin action in man. *The Journal of clinical investigation*. 1984 Apr;73(4):1185-90. PubMed PMID: 6423666.

45. Damsbo P, Vaag A, Hother-Nielsen O, Beck-Nielsen H. Reduced glycogen synthase activity in skeletal muscle from obese patients with and without type 2 (non-insulin-dependent) diabetes mellitus. *Diabetologia*. 1991 Apr;34(4):239-45. PubMed PMID: 1906024.

46. Ducluzeau PH, Perretti N, Laville M, Andreelli F, Vega N, Riou JP, et al. Regulation by insulin of gene expression in human skeletal muscle and adipose tissue. Evidence for specific defects in type 2 diabetes. *Diabetes*. 2001 May;50(5):1134-42. PubMed PMID: 11334418.

47. Gurley JM, Griesel BA, Olson AL. Erratum. Increased Skeletal Muscle GLUT4 Expression in Obese Mice After Voluntary Wheel Running Exercise Is Posttranscriptional.

Diabetes 2016;65:2911-2919. Diabetes. 2016 Dec;65(12):3812. PubMed PMID: 27797913.

48. Schwenk RW, Vogel H, Schurmann A. Genetic and epigenetic control of metabolic health. *Molecular metabolism*. 2013 Sep 25;2(4):337-47. PubMed PMID: 24327950.

49. Han Z, Niu T, Chang J, Lei X, Zhao M, Wang Q, et al. Crystal structure of the FTO protein reveals basis for its substrate specificity. *Nature*. 2010 Apr 22;464(7292):1205-9. PubMed PMID: 20376003.

50. Fani L, Bak S, Delhanty P, van Rossum EF, van den Akker EL. The melanocortin-4 receptor as target for obesity treatment: a systematic review of emerging pharmacological therapeutic options. *International journal of obesity*. 2014 Feb;38(2):163-9. PubMed PMID: 23774329.

51. Michaud EJ, Bultman SJ, Klebig ML, van Vugt MJ, Stubbs LJ, Russell LB, et al. A molecular model for the genetic and phenotypic characteristics of the mouse lethal yellow (Ay) mutation. *Proceedings of the National Academy of Sciences of the United States of America*. 1994 Mar 29;91(7):2562-6. PubMed PMID: 8146154.

52. Ollmann MM, Wilson BD, Yang YK, Kerns JA, Chen Y, Gantz I, et al. Antagonism of central melanocortin receptors in vitro and in vivo by agouti-related protein. *Science*. 1997 Oct 3;278(5335):135-8. PubMed PMID: 9311920.

53. Chen F, Law SW, O'Malley BW. Identification of two mPPAR related receptors and evidence for the existence of five subfamily members. *Biochemical and biophysical research communications*. 1993 Oct 29;196(2):671-7. PubMed PMID: 8240342.

54. Evans RM, Barish GD, Wang YX. PPARs and the complex journey to obesity. *Nature medicine*. 2004 Apr;10(4):355-61. PubMed PMID: 15057233.

55. Tontonoz P, Spiegelman BM. Fat and beyond: the diverse biology of PPAR γ . *Annual review of biochemistry*. 2008;77:289-312. PubMed PMID: 18518822.
56. Glass CK, Saijo K. Nuclear receptor transrepression pathways that regulate inflammation in macrophages and T cells. *Nature reviews Immunology*. 2010 May;10(5):365-76. PubMed PMID: 20414208.
57. Pascual G, Fong AL, Ogawa S, Gamliel A, Li AC, Perissi V, et al. A SUMOylation-dependent pathway mediates transrepression of inflammatory response genes by PPAR- γ . *Nature*. 2005 Sep 29;437(7059):759-63. PubMed PMID: 16127449.
58. Toubal A, Clement K, Fan R, Ancel P, Pelloux V, Rouault C, et al. SMRT-GPS2 corepressor pathway dysregulation coincides with obesity-linked adipocyte inflammation. *The Journal of clinical investigation*. 2013 Jan;123(1):362-79. PubMed PMID: 23221346.
59. Pettersson AT, Mejhert N, Jernas M, Carlsson LM, Dahlman I, Laurencikiene J, et al. Twist1 in human white adipose tissue and obesity. *The Journal of clinical endocrinology and metabolism*. 2011 Jan;96(1):133-41. PubMed PMID: 20943789.
60. Pettersson AT, Laurencikiene J, Mejhert N, Naslund E, Bouloumie A, Dahlman I, et al. A possible inflammatory role of twist1 in human white adipocytes. *Diabetes*. 2010 Mar;59(3):564-71. PubMed PMID: 20007935.
61. Huang ZQ, Li J, Sachs LM, Cole PA, Wong J. A role for cofactor-cofactor and cofactor-histone interactions in targeting p300, SWI/SNF and Mediator for transcription. *The EMBO journal*. 2003 May 1;22(9):2146-55. PubMed PMID: 12727881.
62. Zhong H, May MJ, Jimi E, Ghosh S. The phosphorylation status of nuclear NF- κ B determines its association with CBP/p300 or HDAC-1. *Molecular cell*. 2002 Mar;9(3):625-36. PubMed PMID: 11931769.

63. Jakobsson T, Venteclef N, Toresson G, Damdimopoulos AE, Ehrlund A, Lou X, et al. GPS2 is required for cholesterol efflux by triggering histone demethylation, LXR recruitment, and coregulator assembly at the ABCG1 locus. *Molecular cell*. 2009 May 14;34(4):510-8. PubMed PMID: 19481530.
64. Bannister AJ, Kouzarides T. Regulation of chromatin by histone modifications. *Cell research*. 2011 Mar;21(3):381-95. PubMed PMID: 21321607.
65. Tateishi K, Okada Y, Kallin EM, Zhang Y. Role of Jhdm2a in regulating metabolic gene expression and obesity resistance. *Nature*. 2009 Apr 9;458(7239):757-61. PubMed PMID: 19194461.
66. Bouchard L, Rabasa-Lhoret R, Faraj M, Lavoie ME, Mill J, Perusse L, et al. Differential epigenomic and transcriptomic responses in subcutaneous adipose tissue between low and high responders to caloric restriction. *The American journal of clinical nutrition*. 2010 Feb;91(2):309-20. PubMed PMID: 19939982.
67. Ronn T, Volkov P, Davegardh C, Dayeh T, Hall E, Olsson AH, et al. A six months exercise intervention influences the genome-wide DNA methylation pattern in human adipose tissue. *PLoS genetics*. 2013 Jun;9(6):e1003572. PubMed PMID: 23825961.
68. Qureshi IA, Mehler MF. Emerging roles of non-coding RNAs in brain evolution, development, plasticity and disease. *Nature reviews Neuroscience*. 2012 Jul 20;13(8):528-41. PubMed PMID: 22814587.
69. Sherwin RS. Role of the liver in glucose homeostasis. *Diabetes care*. 1980 Mar-Apr;3(2):261-5. PubMed PMID: 6993137.
70. Bloomgarden ZT. Nonalcoholic fatty liver disease and insulin resistance in youth. *Diabetes care*. 2007 Jun;30(6):1663-9. PubMed PMID: 17526824.
71. Sookoian S, Rosselli MS, Gemma C, Burgueno AL, Fernandez Gianotti T, Castano GO, et al. Epigenetic regulation of insulin resistance in nonalcoholic fatty liver

disease: impact of liver methylation of the peroxisome proliferator-activated receptor gamma coactivator 1alpha promoter. *Hepatology*. 2010 Dec;52(6):1992-2000. PubMed PMID: 20890895.

72. Kershaw EE, Flier JS. Adipose tissue as an endocrine organ. *The Journal of clinical endocrinology and metabolism*. 2004 Jun;89(6):2548-56. PubMed PMID: 15181022.

73. Yokomori N, Tawata M, Onaya T. DNA demethylation during the differentiation of 3T3-L1 cells affects the expression of the mouse GLUT4 gene. *Diabetes*. 1999 Apr;48(4):685-90. PubMed PMID: 10102682.

74. Marin-Juez R, Diaz M, Morata J, Planas JV. Correction: Mechanisms Regulating GLUT4 Transcription in Skeletal Muscle Cells Are Highly Conserved across Vertebrates. *PloS one*. 2014;9(1). PubMed PMID: 29294484.

75. Esteves JV, Enguita FJ, Machado UF. MicroRNAs-Mediated Regulation of Skeletal Muscle GLUT4 Expression and Translocation in Insulin Resistance. *Journal of diabetes research*. 2017;2017:7267910. PubMed PMID: 28428964.

76. Lavebratt C, Almgren M, Ekstrom TJ. Epigenetic regulation in obesity. *International journal of obesity*. 2012 Jun;36(6):757-65. PubMed PMID: 21912396.

77. Widiker S, Karst S, Wagener A, Brockmann GA. High-fat diet leads to a decreased methylation of the Mc4r gene in the obese BFMI and the lean B6 mouse lines. *Journal of applied genetics*. 2010;51(2):193-7. PubMed PMID: 20453306.

78. Plagemann A, Harder T, Brunn M, Harder A, Roepke K, Wittrock-Staar M, et al. Hypothalamic proopiomelanocortin promoter methylation becomes altered by early overfeeding: an epigenetic model of obesity and the metabolic syndrome. *The Journal of physiology*. 2009 Oct 15;587(Pt 20):4963-76. PubMed PMID: 19723777.

79. Stepanow S, Reichwald K, Huse K, Gausmann U, Nebel A, Rosenstiel P, et al. Allele-specific, age-dependent and BMI-associated DNA methylation of human MCHR1. *PloS one*. 2011;6(5):e17711. PubMed PMID: 21637341.
80. Campion J, Milagro F, Martinez JA. Epigenetics and obesity. *Progress in molecular biology and translational science*. 2010;94:291-347. PubMed PMID: 21036330.
81. Ortega FJ, Moreno-Navarrete JM, Pardo G, Sabater M, Hummel M, Ferrer A, et al. MiRNA expression profile of human subcutaneous adipose and during adipocyte differentiation. *PloS one*. 2010 Feb 2;5(2):e9022. PubMed PMID: 20126310.
82. Heude B, Kettaneh A, Rakotovoao R, Bresson JL, Borys JM, Ducimetiere P, et al. Anthropometric relationships between parents and children throughout childhood: the Fleurbaix-Laventie Ville Sante Study. *International journal of obesity*. 2005 Oct;29(10):1222-9. PubMed PMID: 15795752.
83. Magarey AM, Daniels LA, Boulton TJ, Cockington RA. Predicting obesity in early adulthood from childhood and parental obesity. *International journal of obesity and related metabolic disorders : journal of the International Association for the Study of Obesity*. 2003 Apr;27(4):505-13. PubMed PMID: 12664084.
84. Freedman DS, Mei Z, Srinivasan SR, Berenson GS, Dietz WH. Cardiovascular risk factors and excess adiposity among overweight children and adolescents: the Bogalusa Heart Study. *The Journal of pediatrics*. 2007 Jan;150(1):12-7 e2. PubMed PMID: 17188605.
85. Bass R, Eneli I. Severe childhood obesity: an under-recognised and growing health problem. *Postgraduate medical journal*. 2015 Nov;91(1081):639-45. PubMed PMID: 26338983.
86. Nehus E. Obesity and chronic kidney disease. *Current opinion in pediatrics*. 2018 Jan 17. (2):241-246 PubMed PMID: 29346138.

87. Talens RP, Boomsma DI, Tobi EW, Kremer D, Jukema JW, Willemsen G, et al. Variation, patterns, and temporal stability of DNA methylation: considerations for epigenetic epidemiology. *FASEB journal : official publication of the Federation of American Societies for Experimental Biology*. 2010 Sep;24(9):3135-44. PubMed PMID: 20385621.
88. Feinberg AP, Irizarry RA, Fradin D, Aryee MJ, Murakami P, Aspelund T, et al. Personalized epigenomic signatures that are stable over time and covary with body mass index. *Science translational medicine*. 2010 Sep 15;2(49):49ra67. PubMed PMID: 20844285.
89. O'Hara A, Lim FL, Mazzatti DJ, Trayhurn P. Microarray analysis identifies matrix metalloproteinases (MMPs) as key genes whose expression is up-regulated in human adipocytes by macrophage-conditioned medium. *Pflugers Archiv : European journal of physiology*. 2009 Oct;458(6):1103-14. PubMed PMID: 19585142.
90. Gillman MW, Rifas-Shiman S, Berkey CS, Field AE, Colditz GA. Maternal gestational diabetes, birth weight, and adolescent obesity. *Pediatrics*. 2003 Mar;111(3):e221-6. PubMed PMID: 12612275.
91. Taylor PD, Samuelsson AM, Poston L. Maternal obesity and the developmental programming of hypertension: a role for leptin. *Acta physiologica*. 2014 Mar;210(3):508-23. PubMed PMID: 24433239.
92. Gemma C, Sookoian S, Alvarinas J, Garcia SI, Quintana L, Kanevsky D, et al. Maternal pregestational BMI is associated with methylation of the PPARGC1A promoter in newborns. *Obesity*. 2009 May;17(5):1032-9. PubMed PMID: 19148128.
93. Yokomizo H, Inoguchi T, Sonoda N, Sakaki Y, Maeda Y, Inoue T, et al. Maternal high-fat diet induces insulin resistance and deterioration of pancreatic beta-cell function in adult offspring with sex differences in mice. *American journal of physiology Endocrinology and metabolism*. 2014 May 15;306(10):E1163-75. PubMed PMID: 24691028.

94. Waller DK, Mills JL, Simpson JL, Cunningham GC, Conley MR, Lassman MR, et al. Are obese women at higher risk for producing malformed offspring? *American journal of obstetrics and gynecology*. 1994 Feb;170(2):541-8. PubMed PMID: 8116710.
95. Begum G, Stevens A, Smith EB, Connor K, Challis JR, Bloomfield F, et al. Epigenetic changes in fetal hypothalamic energy regulating pathways are associated with maternal undernutrition and twinning. *FASEB journal : official publication of the Federation of American Societies for Experimental Biology*. 2012 Apr;26(4):1694-703. PubMed PMID: 22223754.
96. Ng SF, Lin RC, Laybutt DR, Barres R, Owens JA, Morris MJ. Chronic high-fat diet in fathers programs beta-cell dysfunction in female rat offspring. *Nature*. 2010 Oct 21;467(7318):963-6. PubMed PMID: 20962845.
97. Wei Y, Yang CR, Wei YP, Zhao ZA, Hou Y, Schatten H, et al. Paternally induced transgenerational inheritance of susceptibility to diabetes in mammals. *Proceedings of the National Academy of Sciences of the United States of America*. 2014 Feb 4;111(5):1873-8. PubMed PMID: 24449870.
98. Fullston T, Palmer NO, Owens JA, Mitchell M, Bakos HW, Lane M. Diet-induced paternal obesity in the absence of diabetes diminishes the reproductive health of two subsequent generations of mice. *Human reproduction*. 2012 May;27(5):1391-400. PubMed PMID: 22357767.
99. Morita S, Horii T, Kimura M, Arai Y, Kamei Y, Ogawa Y, et al. Paternal allele influences high fat diet-induced obesity. *PloS one*. 2014;9(1):e85477. PubMed PMID: 24416415.
100. Fullston T, Ohlsson Teague EM, Palmer NO, DeBlasio MJ, Mitchell M, Corbett M, et al. Paternal obesity initiates metabolic disturbances in two generations of mice with incomplete penetrance to the F2 generation and alters the transcriptional profile of testis and sperm microRNA content. *FASEB journal : official publication of the Federation of*

American Societies for Experimental Biology. 2013 Oct;27(10):4226-43. PubMed PMID: 23845863.

101. Denham J, Marques FZ, O'Brien BJ, Charchar FJ. Exercise: putting action into our epigenome. *Sports medicine*. 2014 Feb;44(2):189-209. PubMed PMID: 24163284.

102. Martinez JA, Milagro FI, Claycombe KJ, Schalinske KL. Epigenetics in adipose tissue, obesity, weight loss, and diabetes. *Advances in nutrition*. 2014 Jan 1;5(1):71-81. PubMed PMID: 24425725.

103. Symonds ME, Pope M, Sharkey D, Budge H. Adipose tissue and fetal programming. *Diabetologia*. 2012 Jun;55(6):1597-606. PubMed PMID: 22402988.

104. Hotamisligil GS, Arner P, Caro JF, Atkinson RL, Spiegelman BM. Increased adipose tissue expression of tumor necrosis factor-alpha in human obesity and insulin resistance. *The Journal of clinical investigation*. 1995 May;95(5):2409-15. PubMed PMID: 7738205.

105. Gilbert CA, Slingerland JM. Cytokines, obesity, and cancer: new insights on mechanisms linking obesity to cancer risk and progression. *Annual review of medicine*. 2013;64:45-57. PubMed PMID: 23121183.

106. Cai D, Yuan M, Frantz DF, Melendez PA, Hansen L, Lee J, et al. Local and systemic insulin resistance resulting from hepatic activation of IKK-beta and NF-kappaB. *Nature medicine*. 2005 Feb;11(2):183-90. PubMed PMID: 15685173.

107. Ehses JA, Perren A, Eppler E, Ribaux P, Pospisilik JA, Maor-Cahn R, et al. Increased number of islet-associated macrophages in type 2 diabetes. *Diabetes*. 2007 Sep;56(9):2356-70. PubMed PMID: 17579207.

108. Stephens JM, Lee J, Pilch PF. Tumor necrosis factor-alpha-induced insulin resistance in 3T3-L1 adipocytes is accompanied by a loss of insulin receptor substrate-1

and GLUT4 expression without a loss of insulin receptor-mediated signal transduction. *The Journal of biological chemistry*. 1997 Jan 10;272(2):971-6. PubMed PMID: 8995390.

109. Boura-Halfon S, Zick Y. Phosphorylation of IRS proteins, insulin action, and insulin resistance. *American journal of physiology Endocrinology and metabolism*. 2009 Apr;296(4):E581-91. PubMed PMID: 18728222.

110. Shen W, Wang C, Xia L, Fan C, Dong H, Deckelbaum RJ, et al. Epigenetic modification of the leptin promoter in diet-induced obese mice and the effects of N-3 polyunsaturated fatty acids. *Scientific reports*. 2014 Jun 13;4:5282. PubMed PMID: 24923522.

111. Pham TX, Lee JY. Epigenetic Regulation of Adipokines. *International journal of molecular sciences*. 2017 Aug 10;18(8). PubMed PMID: 28796178.

112. Masuyama H, Hiramatsu Y. Additive effects of maternal high fat diet during lactation on mouse offspring. *PloS one*. 2014;9(3):e92805. PubMed PMID: 24664181.

113. Kim AY, Park YJ, Pan X, Shin KC, Kwak SH, Bassas AF, et al. Obesity-induced DNA hypermethylation of the adiponectin gene mediates insulin resistance. *Nature communications*. 2015 Jul 3;6:7585. PubMed PMID: 26139044.

114. Tain YL, Hsu CN, Chan JY. PPARs Link Early Life Nutritional Insults to Later Programmed Hypertension and Metabolic Syndrome. *International journal of molecular sciences*. 2015 Dec 24;17(1). PubMed PMID: 26712739.

115. Ng SF, Lin RC, Maloney CA, Youngson NA, Owens JA, Morris MJ. Paternal high-fat diet consumption induces common changes in the transcriptomes of retroperitoneal adipose and pancreatic islet tissues in female rat offspring. *FASEB journal : official publication of the Federation of American Societies for Experimental Biology*. 2014 Apr;28(4):1830-41. PubMed PMID: 24421403.

116. Pratipanawatr W, Pratipanawatr T, Cusi K, Berria R, Adams JM, Jenkinson CP, et al. Skeletal muscle insulin resistance in normoglycemic subjects with a strong family history of type 2 diabetes is associated with decreased insulin-stimulated insulin receptor substrate-1 tyrosine phosphorylation. *Diabetes*. 2001 Nov;50(11):2572-8. PubMed PMID: 11679436.
117. Zierath JR, Houseknecht KL, Gnudi L, Kahn BB. High-fat feeding impairs insulin-stimulated GLUT4 recruitment via an early insulin-signaling defect. *Diabetes*. 1997 Feb;46(2):215-23. PubMed PMID: 9000697.
118. Hansen PA, Han DH, Marshall BA, Nolte LA, Chen MM, Mueckler M, et al. A high fat diet impairs stimulation of glucose transport in muscle. Functional evaluation of potential mechanisms. *The Journal of biological chemistry*. 1998 Oct 2;273(40):26157-63. PubMed PMID: 9748297.
119. Xu PT, Song Z, Zhang WC, Jiao B, Yu ZB. Impaired translocation of GLUT4 results in insulin resistance of atrophic soleus muscle. *BioMed research international*. 2015;2015:291987. PubMed PMID: 25713812.
120. Gao L, Chen J, Gao J, Wang H, Xiong W. Super-resolution microscopy reveals the insulin-resistance-regulated reorganization of GLUT4 on plasma membranes. *Journal of cell science*. 2017 Jan 15;130(2):396-405. PubMed PMID: 27888215.
121. Laker RC, Lillard TS, Okutsu M, Zhang M, Hoehn KL, Connelly JJ, et al. Exercise prevents maternal high-fat diet-induced hypermethylation of the Pgc-1alpha gene and age-dependent metabolic dysfunction in the offspring. *Diabetes*. 2014 May;63(5):1605-11. PubMed PMID: 24430439.
122. McMillin SL, Schmidt DL, Kahn BB, Witczak CA. GLUT4 Is Not Necessary for Overload-Induced Glucose Uptake or Hypertrophic Growth in Mouse Skeletal Muscle. *Diabetes*. 2017 Jun;66(6):1491-500. PubMed PMID: 28279980.

123. Ciaraldi TP, Mudaliar S, Barzin A, Macievic JA, Edelman SV, Park KS, et al. Skeletal muscle GLUT1 transporter protein expression and basal leg glucose uptake are reduced in type 2 diabetes. *The Journal of clinical endocrinology and metabolism*. 2005 Jan;90(1):352-8. PubMed PMID: 15483099.

124. Pinhas-Hamiel O, Lerner-Geva L, Copperman N, Jacobson MS. Insulin resistance and parental obesity as predictors to response to therapeutic life style change in obese children and adolescents 10-18 years old. *The Journal of adolescent health : official publication of the Society for Adolescent Medicine*. 2008 Nov;43(5):437-43. PubMed PMID: 18848671.

125. O'Byrne KJ, Baird AM, Kilmartin L, Leonard J, Sacevich C, Gray SG. Epigenetic regulation of glucose transporters in non-small cell lung cancer. *Cancers*. 2011 Mar 25;3(2):1550-65. PubMed PMID: 24212773.

126. Barres R, Zierath JR. DNA methylation in metabolic disorders. *The American journal of clinical nutrition*. 2011 Apr;93(4):897S-900. PubMed PMID: 21289222.

127. Zhang YZ, Slyvka Y, Zontini A, Consitt LA, Heh V and Nowak FV. Effects of Paternal Preconception High Fat Diet on Metabolism and Behavior of Offspring. In review. 2018.

128. Sparks LM, Xie H, Koza RA, Mynatt R, Hulver MW, Bray GA, et al. A high-fat diet coordinately downregulates genes required for mitochondrial oxidative phosphorylation in skeletal muscle. *Diabetes*. 2005 Jul;54(7):1926-33. PubMed PMID: 15983191.

129. DeFronzo RA, Tripathy D. Skeletal muscle insulin resistance is the primary defect in type 2 diabetes. *Diabetes care*. 2009 Nov;32 Suppl 2:S157-63. PubMed PMID: 19875544.

130. Gallou-Kabani C, Junien C. Nutritional epigenomics of metabolic syndrome: new perspective against the epidemic. *Diabetes*. 2005 Jul;54(7):1899-906. PubMed PMID: 15983188.
131. Dudley KJ, Sloboda DM, Connor KL, Beltrand J, Vickers MH. Offspring of mothers fed a high fat diet display hepatic cell cycle inhibition and associated changes in gene expression and DNA methylation. *PloS one*. 2011;6(7):e21662. PubMed PMID: 21779332.
132. Davie JR. Inhibition of histone deacetylase activity by butyrate. *The Journal of nutrition*. 2003 Jul;133(7 Suppl):2485S-93S. PubMed PMID: 12840228.
133. Safdar A, Little JP, Stokl AJ, Hettinga BP, Akhtar M, Tarnopolsky MA. Exercise increases mitochondrial PGC-1alpha content and promotes nuclear-mitochondrial cross-talk to coordinate mitochondrial biogenesis. *The Journal of biological chemistry*. 2011 Mar 25;286(12):10605-17. PubMed PMID: 21245132.
134. Smith BK, Mukai K, Lally JS, Maher AC, Gurd BJ, Heigenhauser GJ, et al. AMP-activated protein kinase is required for exercise-induced peroxisome proliferator-activated receptor co-activator 1 translocation to subsarcolemmal mitochondria in skeletal muscle. *The Journal of physiology*. 2013 Mar 15;591(6):1551-61. PubMed PMID: 23297307.
135. Henagan TM, Stefanska B, Fang Z, Navard AM, Ye J, Lenard NR, et al. Sodium butyrate epigenetically modulates high-fat diet-induced skeletal muscle mitochondrial adaptation, obesity and insulin resistance through nucleosome positioning. *British journal of pharmacology*. 2015 Jun;172(11):2782-98. PubMed PMID: 25559882.
136. Pertea M, Kim D, Pertea GM, Leek JT, Salzberg SL. Transcript-level expression analysis of RNA-seq experiments with HISAT, StringTie and Ballgown. *Nature protocols*. 2016 Sep;11(9):1650-67. PubMed PMID: 27560171.
137. Singer JD, Willett JB. *Applied Longitudinal Data Analysis: Modelling Change and Event Occurrence*. New York, NY: Oxford University Press; 2003.

138. Obrochta KM, Krois CR, Campos B, Napoli JL. Insulin regulates retinol dehydrogenase expression and all-trans-retinoic acid biosynthesis through FoxO1. *The Journal of biological chemistry*. 2015 Mar 13;290(11):7259-68. PubMed PMID: 25627686.
139. Liden M, Eriksson U. Understanding retinol metabolism: structure and function of retinol dehydrogenases. *The Journal of biological chemistry*. 2006 May 12;281(19):13001-4. PubMed PMID: 16428379.
140. Gluckman PD, Hanson MA. Developmental and epigenetic pathways to obesity: an evolutionary-developmental perspective. *International journal of obesity*. 2008 Dec;32 Suppl 7:S62-71. PubMed PMID: 19136993.
141. Smith U, Kahn BB. Adipose tissue regulates insulin sensitivity: role of adipogenesis, de novo lipogenesis and novel lipids. *Journal of internal medicine*. 2016 Nov;280(5):465-75. PubMed PMID: 27699898.
142. Peng J, Wu Y, Deng Z, Zhou Y, Song T, Yang Y, et al. MiR-377 promotes white adipose tissue inflammation and decreases insulin sensitivity in obesity via suppression of sirtuin-1 (SIRT1). *Oncotarget*. 2017 Sep 19;8(41):70550-63. PubMed PMID: 29050301.
143. Consitt LA, Saxena G, Slyvka Y, Friedlander M, Zhang Y, Nowak FV. Paternal high fat diet enhances offspring whole-body insulin sensitivity and skeletal muscle insulin signaling early in life. *Physiological Reports* (In Press).
144. Barros RP, Machado UF, Warner M, Gustafsson JA. Muscle GLUT4 regulation by estrogen receptors ERbeta and ERalpha. *Proceedings of the National Academy of Sciences of the United States of America*. 2006 Jan 31;103(5):1605-8. PubMed PMID: 16423895.
145. Zheng S, Rollet M, Pan YX. Protein restriction during gestation alters histone modifications at the glucose transporter 4 (GLUT4) promoter region and induces GLUT4 expression in skeletal muscle of female rat offspring. *The Journal of nutritional biochemistry*. 2012 Sep;23(9):1064-71. PubMed PMID: 22079207.

146. Shan WF, Chen BQ, Zhu SJ, Jiang L, Zhou YF. Effects of GLUT4 expression on insulin resistance in patients with advanced liver cirrhosis. *Journal of Zhejiang University Science B*. 2011 Aug;12(8):677-82. PubMed PMID: 21796809.
147. Garvey WT, Maianu L, Zhu JH, Brechtel-Hook G, Wallace P, Baron AD. Evidence for defects in the trafficking and translocation of GLUT4 glucose transporters in skeletal muscle as a cause of human insulin resistance. *The Journal of clinical investigation*. 1998 Jun 1;101(11):2377-86. PubMed PMID: 9616209.
148. Yan ST, Li CL, Tian H, Li J, Pei Y, Liu Y, et al. MiR-199a is overexpressed in plasma of type 2 diabetes patients which contributes to type 2 diabetes by targeting GLUT4. *Molecular and cellular biochemistry*. 2014 Dec;397(1-2):45-51. PubMed PMID: 25084986.
149. Martin S, Millar CA, Lyttle CT, Meerloo T, Marsh BJ, Gould GW, et al. Effects of insulin on intracellular GLUT4 vesicles in adipocytes: evidence for a secretory mode of regulation. *Journal of cell science*. 2000 Oct;113 Pt 19:3427-38. PubMed PMID: 10984434.
150. Bryant NJ, Govers R, James DE. Regulated transport of the glucose transporter GLUT4. *Nature reviews Molecular cell biology*. 2002 Apr;3(4):267-77. PubMed PMID: 11994746.
151. Whitaker RC, Wright JA, Pepe MS, Seidel KD, Dietz WH. Predicting obesity in young adulthood from childhood and parental obesity. *The New England journal of medicine*. 1997 Sep 25;337(13):869-73. PubMed PMID: 9302300.
152. Pembrey ME, Bygren LO, Kaati G, Edvinsson S, Northstone K, Sjöström M, et al. Sex-specific, male-line transgenerational responses in humans. *European journal of human genetics : EJHG*. 2006 Feb;14(2):159-66. PubMed PMID: 16391557.
153. Veena SR, Krishnaveni GV, Karat SC, Osmond C, Fall CH. Testing the fetal overnutrition hypothesis; the relationship of maternal and paternal adiposity to adiposity,

insulin resistance and cardiovascular risk factors in Indian children. *Public health nutrition*. 2013 Sep;16(9):1656-66. PubMed PMID: 22895107.

154. Wei Y, Schatten H, Sun QY. Environmental epigenetic inheritance through gametes and implications for human reproduction. *Human reproduction update*. 2015 Mar-Apr;21(2):194-208. PubMed PMID: 25416302.

155. Terashima M, Barbour S, Ren J, Yu W, Han Y, Muegge K. Effect of high fat diet on paternal sperm histone distribution and male offspring liver gene expression. *Epigenetics*. 2015;10(9):861-71. PubMed PMID: 26252449.

156. Soubry A, Murphy SK, Wang F, Huang Z, Vidal AC, Fuemmeler BF, et al. Newborns of obese parents have altered DNA methylation patterns at imprinted genes. *International journal of obesity*. 2015 Apr;39(4):650-7. PubMed PMID: 24158121.

157. Carone BR, Fauquier L, Habib N, Shea JM, Hart CE, Li R, et al. Paternally induced transgenerational environmental reprogramming of metabolic gene expression in mammals. *Cell*. 2010 Dec 23;143(7):1084-96. PubMed PMID: 21183072.

158. Chen Q, Yan M, Cao Z, Li X, Zhang Y, Shi J, et al. Sperm tsRNAs contribute to intergenerational inheritance of an acquired metabolic disorder. *Science*. 2016 Jan 22;351(6271):397-400. PubMed PMID: 26721680.

159. Grandjean V, Fourre S, De Abreu DA, Derieppe MA, Remy JJ, Rassoulzadegan M. RNA-mediated paternal heredity of diet-induced obesity and metabolic disorders. *Scientific reports*. 2015 Dec 14;5:18193. PubMed PMID: 26658372.

160. McPherson NO, Fullston T, Aitken RJ, Lane M. Paternal obesity, interventions, and mechanistic pathways to impaired health in offspring. *Annals of nutrition & metabolism*. 2014;64(3-4):231-8. PubMed PMID: 25300265.

161. Fullston T, McPherson NO, Owens JA, Kang WX, Sandeman LY, Lane M. Paternal obesity induces metabolic and sperm disturbances in male offspring that are

exacerbated by their exposure to an "obesogenic" diet. *Physiological reports*. 2015 Mar;3(3). PubMed PMID: 25804263.

162. Kim OK, Jun W, Lee J. Mechanism of ER Stress and Inflammation for Hepatic Insulin Resistance in Obesity. *Annals of nutrition & metabolism*. 2015;67(4):218-27. PubMed PMID: 26452040.

163. Piya MK, McTernan PG, Kumar S. Adipokine inflammation and insulin resistance: the role of glucose, lipids and endotoxin. *The Journal of endocrinology*. 2013 Jan;216(1):T1-T15. PubMed PMID: 23160966.

164. Kwon H, Pessin JE. Adipokines mediate inflammation and insulin resistance. *Frontiers in endocrinology*. 2013;4:71. PubMed PMID: 23781214.

165. Meshkani R, Adeli K. Hepatic insulin resistance, metabolic syndrome and cardiovascular disease. *Clinical biochemistry*. 2009 Sep;42(13-14):1331-46. PubMed PMID: 19501581.

166. Ballak DB, Stienstra R, Tack CJ, Dinarello CA, van Diepen JA. IL-1 family members in the pathogenesis and treatment of metabolic disease: Focus on adipose tissue inflammation and insulin resistance. *Cytokine*. 2015 Oct;75(2):280-90. PubMed PMID: 26194067.

167. Kern PA, Ranganathan S, Li C, Wood L, Ranganathan G. Adipose tissue tumor necrosis factor and interleukin-6 expression in human obesity and insulin resistance. *American journal of physiology Endocrinology and metabolism*. 2001 May;280(5):E745-51. PubMed PMID: 11287357.

168. Rakotoarivelo V, Lacraz G, Mayhue M, Brown C, Rottembourg D, Fradette J, et al. Inflammatory Cytokine Profiles in Visceral and Subcutaneous Adipose Tissues of Obese Patients Undergoing Bariatric Surgery Reveal Lack of Correlation With Obesity or Diabetes. *EBioMedicine*. 2018 Apr;30:237-47. PubMed PMID: 29548899.

169. Tian R, Zuo X, Jaoude J, Mao F, Colby J, Shureiqi I. ALOX15 as a suppressor of inflammation and cancer: Lost in the link. *Prostaglandins & other lipid mediators*. 2017 Sep;132:77-83. PubMed PMID: 28089732.
170. Kwon HJ, Kim SN, Kim YA, Lee YH. The contribution of arachidonate 15-lipoxygenase in tissue macrophages to adipose tissue remodeling. *Cell death & disease*. 2016 Jun 30;7(6):e2285. PubMed PMID: 27362803.
171. Wilson CG, Robert-Cooperman CE, Burkhardt BR. PANcreatic-DERived factor: novel hormone PANDERing to glucose regulation. *FEBS letters*. 2011 Jul 21;585(14):2137-43. PubMed PMID: 21664909.
172. Yang J, Guan Y. Family with sequence similarity 3 gene family and nonalcoholic fatty liver disease. *Journal of gastroenterology and hepatology*. 2013 Aug;28 Suppl 1:105-11. PubMed PMID: 23855304.
173. Zhang X, Yang W, Wang J, Meng Y, Guan Y, Yang J. FAM3 gene family: A promising therapeutical target for NAFLD and type 2 diabetes. *Metabolism: clinical and experimental*. 2018 Apr;81:71-82. PubMed PMID: 29221790.
174. Nishizuka M, Koyanagi A, Osada S, Imagawa M. Wnt4 and Wnt5a promote adipocyte differentiation. *FEBS letters*. 2008 Sep 22;582(21-22):3201-5. PubMed PMID: 18708054.
175. Westermeier F, Saez PJ, Villalobos-Labra R, Sobrevia L, Farias-Jofre M. Programming of fetal insulin resistance in pregnancies with maternal obesity by ER stress and inflammation. *BioMed research international*. 2014;2014:917672. PubMed PMID: 25093191.
176. Resnyk CW, Chen C, Huang H, Wu CH, Simon J, Le Bihan-Duval E, et al. RNA-Seq Analysis of Abdominal Fat in Genetically Fat and Lean Chickens Highlights a Divergence in Expression of Genes Controlling Adiposity, Hemostasis, and Lipid Metabolism. *PloS one*. 2015;10(10):e0139549. PubMed PMID: 26445145.

177. Chu B, Wu T, Miao L, Mei Y, Wu M. MiR-181a regulates lipid metabolism via IDH1. *Scientific reports*. 2015 Mar 5;5:8801. PubMed PMID: 25739786.
178. Carreras-Badosa G, Bonmati A, Ortega FJ, Mercader JM, Guindo-Martinez M, Torrents D, et al. Dysregulation of Placental miRNA in Maternal Obesity Is Associated With Pre- and Postnatal Growth. *The Journal of clinical endocrinology and metabolism*. 2017 Jul 1;102(7):2584-94. PubMed PMID: 28368446.
179. McPherson NO, Lane M, Sandeman L, Owens JA, Fullston T. An Exercise-Only Intervention in Obese Fathers Restores Glucose and Insulin Regulation in Conjunction with the Rescue of Pancreatic Islet Cell Morphology and MicroRNA Expression in Male Offspring. *Nutrients*. 2017 Feb 9;9(2). PubMed PMID: 28208792.
180. Bakos HW, Mitchell M, Setchell BP, Lane M. The effect of paternal diet-induced obesity on sperm function and fertilization in a mouse model. *International journal of andrology*. 2011 Oct;34(5 Pt 1):402-10. PubMed PMID: 20649934.



OHIO
UNIVERSITY

Thesis and Dissertation Services